Physics – Uspekhi **64** (10) 1021 – 1037 (2021)

REVIEWS OF TOPICAL PROBLEMS PACS numbers: 03.65.Ud, **03.67.–a**, 42.50.Ex

Large quantum networks

D D Sukachev

DOI: https://doi.org/10.3367/UFNe.2020.11.038888

Contents

Abstract. Quantum networks that allow generating entangled states between distant qubits have enormous scientific and applied potential. They can be used for secure quantum cryptography and the teleportation of quantum states between cities and countries, in high-resolution astronomy, and in distributed quantum computing. The scattering of photons in an optical fiber and the difficulties in creating full-fledged quantum nodes impede the construction of large quantum networks. We review current approaches to the creation of such networks, with the emphasis on quantum repeaters intended for 'compensating' losses in optical fibers. We also discuss methods for increasing the range of quantum cryptography systems without using quantum repeaters.

Keywords: quantum network, quantum cryptography, quantum repeater

1. Introduction

Over the past century, quantum mechanics, which once was an abstract physical theory, has become the basis for various technologies that we use every day, such as lasers, satellite navigation systems, magnetic resonance imaging, and semiconductor electronics. And yet the application of quantum mechanics to the analysis of many physical, biological, and chemical problems is often limited by the impossibility of calculating the behavior of quantum systems on present-day computers due to the exponential dependence of the required computing power on the quantum system size [1].

D D Sukachev University of Calgary,
2500 University Drive NW, Calgary, AB T2N 1N4, Canada
E-mail: sukachev@gmail.com

Received 9 June 2020, revised 26 November 2020
Uspekhi Fizicheskikh Nauk **191** (10) 1077 – 1094 (2021)
Translated by S Alekseev

To solve such problems, in the 1980s, Manin [2] and Feynman [3] proposed to use *quantum computers* — quantum mechanical systems that can obviate that exponential increase because they store and process information in quantum form. Next, in 1992, Deutsch and Jozsa established that quantum computers can also accelerate the solution to certain mathematical problems [4]. A pivotal event occurred in 1994, when Shor proposed a polynomial-time quantum prime factorization algorithm, which was a huge leap compared with the exponential dependence for the best classical algorithm [5].

The integer factorization problem is of particular importance in the modern world, because it underlies the Rivest–Shamir–Adleman (RSA) algorithm, the most widespread public-key cryptographic system on the Internet (asymmetric encryption) [6], which allows a confidential exchange of information between two users who have not met before or have had the opportunity to agree on a common encryption key [7]. For this, the first user (server) selects two primes, q and r, forms a *public key* $p = qr$ from them, and sends it to the second user (client) via an unprotected communication channel. The client encrypts its message with the public key and sends it back to the server over the same channel. For decryption, the server uses a *secret key* known only to him, which is constructed from q and r.

Thus, the ability of an attacker to decrypt a message directly depends on his ability to factor the public key, which means that one day quantum computers will be able to crack data transmission channels. Due to the enormous complexity of the creation of quantum computers, it has so far been possible to factor only an 8-bit number [8], while factoring a 2048-bit public key (a standard as of 2020) may require more than a million qubits [9]. Existing universal quantum computers have only 50 to 100 qubits [10–12] and will not be able to crack the RSA algorithm in the near future; however, some data transmitted today has to be kept secret for many decades [13].

The problem of protecting telecommunication systems against quantum attacks has at least two solutions. The first is postquantum cryptography [14], relying on mathematical encryption algorithms for which no analogues of the Shor algorithm are known; still, there is no guarantee that the corresponding quantum decryption algorithm cannot be developed in the future. The second solution was found in 1984, when Bennett and Brassard proposed using single photons to generate a *symmetric* secret key for two users (the BB84 protocol); the secrecy of such a key — the fact that it is known to only these two users — is guaranteed by the laws of quantum mechanics [15]. The encryption itself is done with *one-time pads*, in which the message is encrypted by the bitwise 'exclusive or' operation using the secret key [7]. Such an algorithm has *absolute cryptographic strength*: there is no mathematical algorithm capable of decrypting a message without knowing the key. This discovery gave rise to a new discipline, *quantum cryptography*, or, more precisely, *quantum key distribution* (QKD) [16]. QKD systems have now become available commercially. In Russia, they are produced by QRate companies founded by employees of the Russian Quantum Center, and by 'Infotex' in cooperation with the Center for Quantum Technologies of Lomonosov Moscow State University [17]; such systems are in use in some banks [18].

The BB84 algorithm [15] is based on the exchange of classical bits of information encoded in the polarization states of *single photons* in two nonorthogonal bases between two users, Alice and Bob. Evidently, information is transmitted only if the sender's single photon reaches the intended recipient. Therefore, if an attacker intercepts a single photon, it must be measured and resent as an exact copy in order to not betray the attacker, but this is prevented by the *no-cloning theorem* [19] in quantum mechanics. As a result, the attacker cannot reliably know which photon (bit) was sent, and the secrecy of the secret key is not guaranteed by the complexity of calculating some mathematical function but by the laws of physics [16].

The next logical step is to construct sufficiently long-range QKD systems for communication over geographic distances. The main difficulty in this case lies in the absorption and scattering of light, which can be conveniently demonstrated using the discussed BB84 quantum cryptography algorithm (see [16] for technical details). If 10^9 photons per second are sent over 500 km along a commercial optical fiber (which is the most convenient transmission method), only one photon per second can be detected at the other end of the fiber (see Section 4). At the same time, commercial single-photon detectors have approximately the same probability of false hits (the number of dark counts); in other words, half of the bits of the resulting encryption key are incorrect, which makes the key useless [13, 16]. Although the QKD was implemented in an optical fiber 400 km in length in laboratory conditions [20], practical application of existing quantum cryptography systems is still limited to a distance of about 100 km [13].

To solve this problem, *quantum repeaters* were proposed in 1998 [21], capable of 'compensating' the losses due to absorption of photons without violating the no-cloning theorem [21, 22]. Quantum repeaters will allow not only implementing QKD systems at long distances but also creating a *quantum Internet*, or *quantum networks* [23, 24], in which quantum computers sitting in the *network nodes* are interconnected by quantum communication channels. The main purpose of the quantum Internet is the distribution of quantum entanglement between network nodes, which can then be used for distributed [24] and secure cloud quantum computing, where servers process encoded information [25, 26], to increase the angular resolution in astronomy [27, 28]; for a secure distribution of time and frequency signals [29]; to build a global network of atomic clocks with a sensitivity close to the quantum limit [30–32]; and in metrology [33–35]. Of particular interest is the implementation of the *device-independent QKD method* [36], in which network nodes can verify the complete secrecy of the received encryption keys independently by measuring quantum correlations (Bell's inequalities [37]), even if an attacker has access to the quantum network. This is the advantage of the device-independent QKD method over existing commercial QKD systems, which do not use entangled states.

The aim of this review is to discuss recent experimental results to create large-scale quantum networks. In Section 2, we discuss the main components of quantum networks. Section 3 is devoted to an overview of platforms for creating quantum network nodes. Section 4 is devoted to a review of various quantum repeater schemes and experimental results. In Section 5, we describe the conversion of photons from the optical band to the telecommunication band, which is necessary for their efficient transmission over optical fibers. In Section 6, we discuss methods to increase the range of quantum networks without using quantum repeaters.

2. Quantum networks

Just like classical computer networks, quantum networks consist of nodes, communication channels, and end users (Fig. 1). The main purpose of a quantum network is to generate entangled states between qubits located at different nodes or at end users. Building a quantum network requires not only physical devices (nodes and single-photon sources) but also data exchange protocols such as TCP/IP (transfer control protocol/Internet protocol) that are needed in order to connect various devices (for example, quantum computers) to the network without addressing their physical implementation [38]. Let us list the main physical components of a quantum network.

Quantum channel. The communication channel must be able to transfer quantum information between network nodes and end users. Currently, the only candidate for the transmission of quantum information over macroscopic distances is a quantum of light in the visible or near-infrared range, i.e., a photon propagating in free space or inside an optical fiber. To ensure the information security of a communication channel, each bit of quantum informa-

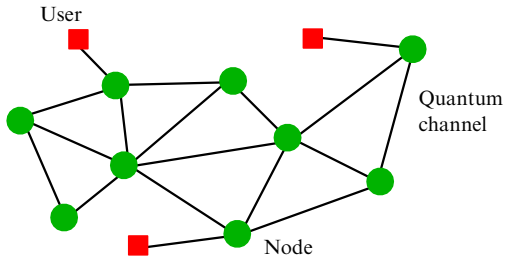

Figure 1. Quantum network in which the nodes (dots) and end users (squares) are connected by quantum communication channels. (Courtesy of B Machielse.)

tion — *qubit* — must be encoded with a single photon [16, 19] (or with a cluster state; see Section 4.2). For this, different parameters of the photon can be used: its polarization, frequency, phase, detection time (time-bin encoding), spatial mode, etc., each of which has its own advantages and disadvantages. We note that phonons (vibrations of the crystal lattice) [39–41] and microwave photons [42] can also be used to build quantum networks within one laboratory, e.g., connecting several quantum computers together. However, they are not suitable for connecting distant quantum nodes: for example, directional propagation of microwaves requires stiff metal waveguides cooled to temperatures of the order of 4 K, which is absolutely impractical.

Single-photon source. Single photons are an important component of quantum networks. For example, the BB84 algorithm, discussed in the Introduction, in its simplest form requires the use of just single photons to encode information. An ideal source must emit a single photon at the push of a button (photon on demand). Among the many different approaches to the creation of such sources [43, 44], of greatest potential are quantum dots in two-dimensional materials [45] and epitaxial (self-assembled) quantum dots in microcavities [46–50].

In 2015, a single-photon source at a wavelength of 1.5 μm was used in quantum cryptography at a distance up to 120 km [51]. But no reliable commercial source of single photons exists yet. Fortunately, in many quantum information protocols, including the BB84 protocol, highly attenuated coherent laser radiation can be used, which makes the probability of detecting two or more photons much less than the probability of detecting a single-photon state. However, in the overwhelming majority of cases, such a laser pulse would not contain any photons at all, and the probability of receiving even one photon would be low, which would significantly slow down the operation of the quantum network. Moreover, the existence of a multiphoton component may allow eavesdropping on the communication channel, which must, of course, be avoided [52, 53]. Thus, the creation of a reliable single-photon source remains an urgent issue, resolving which is necessary for building quantum networks.

Photodetectors. Along with single-photon sources, there are single-photon detectors. The main parameter of these detectors is their quantum efficiency, which shows the probability of a detector triggering when hit by a photon; the dark current, equal to the number of false positives per unit time; and the counting rate [54].

A high quantum efficiency is needed not only to increase the speed of the quantum network (which is obvious) but also for the correct operation of many network nodes. Indeed, after the interaction of a photon with a qubit, they become entangled, and the state of the qubit can become known only after the state of the photon is measured. However, if the photon was lost or the detector 'missed' it, then the qubit state remains unknown and has to be re-initialized [55], and because it is not known at what moment the detector failed, the low quantum efficiency increases the probability of errors in quantum operations (see Section 4). The dark current also increases the probability of error due to the false impression that a photon has been received [16].

Until recently, the single-photon detectors most widely used in quantum optics were photon counters based on avalanche photodiodes, which, in the optical domain, have a sufficiently high quantum efficiency ($> 50\%$) and a low dark current (< 100 photons per second). But in the telecommunication band, which is of greatest interest for quantum networks and QKDs, such counters perform much worse (quantum efficiency $< 20\%$, dark current > 1000 photons per second). Moreover, even a quantum efficiency of about 70% is often insufficient [55]. Recently, detectors based on superconducting nanowires have appeared [56] (in Russia, produced by Skontel) that have a quantum efficiency $> 95\%$ and a dark current < 1 photon per second in both the optical and telecommunication bands [57].

Quantum nodes. A network node is in general realized as a small quantum computer that can store and process quantum information and exchange it with other network nodes. The approaches to quantum information processing and hence to the construction of quantum nodes can be divided into two large groups: those based on unitary reversible quantum logic elements using stationary qubits (atoms, ions, and superconducting qubits; see Section 3) and those based on irreversible measurements of photon cluster states [58–60] (see Section 4.3). A quantum node can perform various functions. For example, it can represent a full-fledged quantum computer with many qubits or an atomic clock connected by a quantum channel with another node responsible for connecting to the quantum network. We discuss here only one specific type of quantum nodes, quantum repeaters, which are necessary for constructing large quantum networks.

Quantum repeater. We mentioned in the Introduction that the scattering and absorption of light impose a constraint on the distance between two nodes that can be directly connected via a communication channel. Let us consider this in more detail. We suppose that a photon must be sent through an optical fiber (the most important method from the applied standpoint). To do so, it is reasonable to use photons with the wavelength of 1550 nm, at which the quartz fiber has the lowest losses $\alpha = 0.18$ dB km^{-1} [61]. Although optical fibers with even lower losses, e.g., 0.14 dB km^{-1}, have been designed [62], they are still commercially unavailable. The probability that the photon does not scatter after passing a distance L along the optical fiber is

$$p_0 = 10^{-\alpha L/10}\,, \tag{1}$$

and is shown in Fig. 2. The exponential dependence in (1) explains why commercial quantum cryptography systems are limited to distances of about 100 km. To make these numbers more descriptive, we suppose that Alice generates entangled pairs of photons at a frequency of 10 GHz (which is the bandwidth of modern optoelectronic devices [63]). For $L = 1000$ km, the mean waiting time for one photon to be received by Bob is then about one year. A radical way to overcome this problem is not to transmit the photon along an optical fiber but through the atmosphere or even via a satellite (see Section 6.1), but this is more expensive and less practical.

There are several ways to increase the bandwidth of a fiber communication channel. For example, wavelength division multiplexing can be used, which consists of transmitting several pulses simultaneously along the same fiber at different wavelengths, which allows increasing the data transfer rate by a factor ~ 100, but still cannot eliminate the exponential dependence in (1). On the other hand, the widely used optical-fiber amplifiers are useless for quantum networks, because quantum mechanics forbids cloning a single photon [19]. In 1998, Briegel, Dür, Cirac, and Zoller (BDCZ) proposed a *quantum repeater* [21] based on quantum teleportation [64] and the exchange of entanglement [65, 66] (the

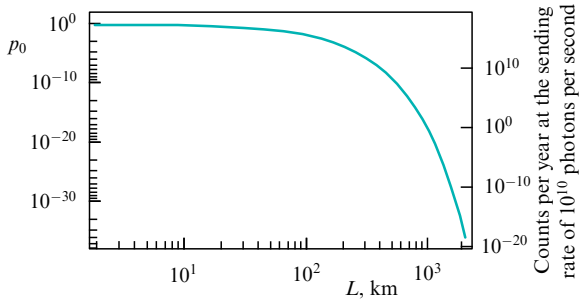

Figure 2. Effect of scattering in an optical fiber on QKD. p_0 is probability of detecting a photon after an optical fiber with the length L and loss of 0.18 dB km^{-1}. Right vertical axis shows number of counts per year when sending 10^{10} photons per second.

BDCZ protocol). The use of quantum repeaters 'compensates' losses in optical fibers and can replace the exponential dependence of the rate of entanglement of remote nodes with a polynomial dependence at the expense of increasing the number of quantum resources. Obviously, a quantum repeater is a particular case of a quantum network node. The BDCZ protocol and its practical implementation are discussed in Section 4.1. Section 4.2 is devoted to a new type of quantum repeater, *one-way quantum repeaters*, which lead to a multiple increase in performance compared to the BDCZ protocol. In Section 4.3, we briefly describe a quantum repeater scheme based on photon cluster states, which does not require permanent quantum memory.

Direct transfer limit. To compare the throughput of quantum networks and demonstrate the advantages of using quantum repeaters, it is convenient to use QKD, which is an important application of such networks. One of the main characteristics of QKD is the *secret key capacity* — the number of the encryption key bits that can be received if one photon is sent. It can be shown that the theoretical upper bound, which we call the *direct transmission limit*, is [67]

$$r_{\mathrm{DT}} = -\log_2(1-p_0) \approx 1.44\,p_0\,. \tag{2}$$

It is obvious that, for the BB84 protocol, the secret key capacity is

$$r_{\mathrm{BB}} = p_0\,. \tag{3}$$

The use of an ideal quantum repeater already results in a significant gain, because the linear dependence on p_0 is superseded by a square-root dependence [68] (see Section 4),

$$r_{\mathrm{QR}} = -\log_2(1-\sqrt{p_0}) \approx 1.44\sqrt{p_0}\,, \tag{4}$$

and several repeaters can ensure a polynomial dependence on the distance L.

Due to the lack of effective quantum repeaters, existing quantum networks are limited to two nodes and distances of the order of several meters or kilometers [71–75] (Fig. 3), but even such relatively simple networks have already been used to test the theory of hidden parameters in quantum mechanics [69, 70]. However, the practical use of these networks, for example, for a device-independent QKD, is still impossible due to the relatively low quality of entangled states or a very low rate of their generation. We also note a recently constructed quantum network based on two superconducting quantum computers spaced 10 m apart and connected by a cryogenic channel for microwave photons (Wallraff's group [42]). Such a network cannot cover an entire city, but it can be useful for building a cluster of quantum computers — a quantum supercomputer.

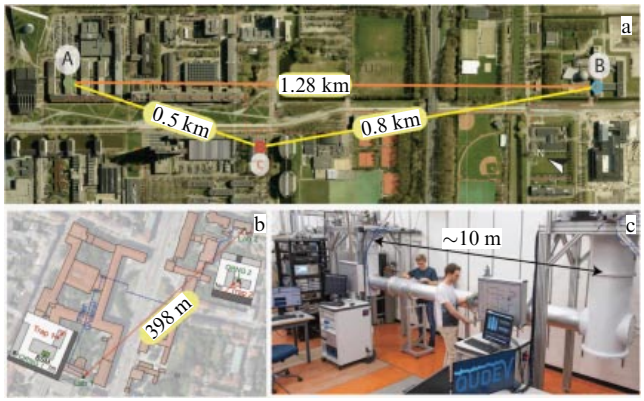

Figure 3. Examples of quantum networks. (a) Aerial photo of the Delft University of Technology campus (The Netherlands). Entangled qubits based on NV centers at points A and B separated by 1.28 km were used to test Bell's inequality. (Reproduced from from [69], with permission from Springer Nature, © 2015.) (b) Map of the Ludwig–Maximilians University campus (Munich, Germany); two single atoms at the distance of 398 m from each other were used to test Bell's inequality [70] (reproduced from [70], published under the Creative Commons Attribution 4.0 International license). (c) A quantum network made of two superconducting qubits placed in different cryostats (Swiss Federal Institute of Technology in Zürich, Switzerland) [42] (reproduced from [42] with permission from the American Physical Society, © 2021).

3. Quantum nodes

Quantum nodes, which are in fact quantum computers, must be capable of storing and processing quantum information and exchanging it with other nodes. The most common and intuitive approach to processing quantum information is based on unitary quantum operations — quantum logical circuits — applied to stationary qubits. (Quantum nodes based on an alternative paradigm involving photon cluster states are discussed in Section 4.3.) One- and two-qubit quantum operations are used in processing quantum information. Their specific implementation depends on the type of qubit; single-qubit operations are mainly carried out via the interaction of a qubit with an external electromagnetic field [76–79]. Acoustic waves can also be used to control solid-state qubits [80, 81], and because such waves interact with almost all solid-state qubits, they are suitable for creating hybrid systems [41] that combine the advantages of different platforms. Interaction with acoustic waves is also used in quantum wavelength converters (see Section 5). Two-qubit operations can be performed by 'switching on' a controlled interaction between qubits [82, 83].

We explicitly list the main requirements for quantum nodes that are needed to build a quantum repeater [84].

(1) The presence of qubits with long-term quantum memory and the possibility of efficient initialization and read-out.

(2) The presence of several qubits per node.

(3) The possibility of carrying out two-qubit operations.

(4) Storing a photon into memory.

(5) Emitting a photon into an optical fiber mode.

(6) Scalability.

Criterion 1 is necessary for storing quantum information, and several qubits (in items 2 and 3) are necessary, for example, for *distilling quantum entanglement* [85] between network nodes, which uses several copies of entangled states (storing which requires several qubits) to create a single state with enhanced characteristics, as is necessary for the efficient operation of quantum repeaters (see Section 4.1). Interaction with single photons (items 4 and 5) serves for communication with neighboring nodes, and scalability (criterion 6) is needed for commercialization.

We note that the fulfillment of all these criteria does not guarantee, for example, that a quantum repeater will give a practical gain in speed in quantum cryptography tasks (see Section 4.1.2). There are currently many platforms satisfying some of the specified criteria, but no system has been constructed to combine all these properties. Some criteria can be relaxed in the case of specialized quantum nodes; for example, several one-way quantum repeater protocols do not require long-term quantum memory [86] (see Section 4.2).

Based on criteria 4 and 5, two groups of qubits can be distinguished: those coherently interacting with light in the optical or infrared band (atoms and ions) and noninteracting ones (superconducting qubits). The latter require quantum transducers, which are still far from perfect, despite significant progress in this area [87, 88] (see Section 5). In what follows, we discuss only qubits interacting with light. They can be divided into two large subgroups: qubits based on atoms and ions in traps [89] and solid-state qubits (color centers and quantum dots) [90].

Although neutral atoms and ions are promising platforms for quantum simulations [91, 92], the complexity of experimental facilities makes them unsuitable for widespread use [93, 94] (which violates criterion 5). But atom and ion traps on chips with integrated cavities [95, 96] are worthy of note: they have practical potential for quantum networks. Also, the presence of narrow clock transitions in atoms may allow building a quantum network of optical clocks [30–32].

The most interesting from the practical standpoint are solid-state qubits that can be integrated on a chip with single-photon sources, photodetectors, and nanophotonic optical elements [97, 98]. Such systems are much simpler and more reliable than atomic traps, and they can in principle be produced at scale (criterion 6). At the same time, satisfying criteria 1–3 depends on the specific qubit type and does not have a universal solution.

3.1 Optical cavities

For the above criteria 4 and 5 to be satisfied, a deterministic interaction between a qubit and a photon is required, but the cross section of photon scattering by an isolated qubit is too small for that. The common method for solving this problem is to place a qubit into an optical cavity, where, due to multiple reflection of a photon from mirrors, the probability of its interaction with the qubit increases $\propto Q/V$ times (the Purcell effect), where Q is the quality factor of the cavity and V is the cavity mode volume [99–101]. It is therefore desirable to have a high-Q cavity with the shortest possible length.

In Fig. 4, we show different variants of cavities. The Fabry–Perot cavity with two dielectric mirrors (Fig. 4a) is used in experiments with neutral atoms [95, 102] and color centers in solids [103–105], and, although its Q-factor can be quite high, it is rather difficult to achieve a small volume of the mode and stabilize the cavity length. Working with solid-state qubits allows cavities to be made from Bragg mirrors or

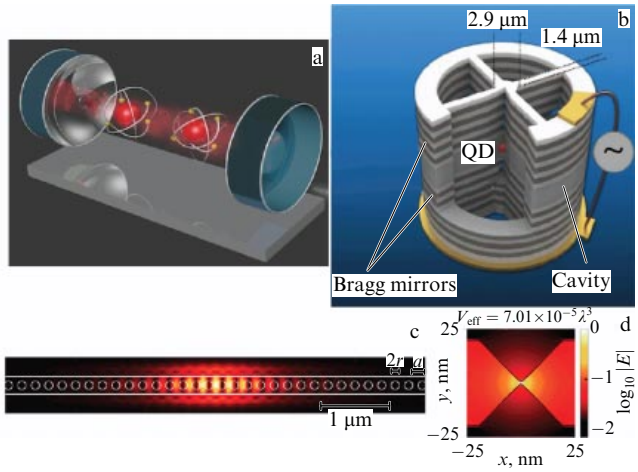

Figure 4. Optical cavities. (a) Fabry–Perot cavity with two spatially separated mirrors (courtesy of © St. Welte, Max Planck Institute of Quantum Optics). (b) Microcavity with Bragg mirrors (reproduced from [108], published under the Creative Commons CC BY license). (c) Photonic-crystal cavity (reproduced from [109] with permission from AIP Publishing, © 2017). (d) Cavity with a very small mode volume (reproduced from [106] with permission from the American Physical Society, © 2017).

photonic crystals (Fig. 4b, c) with integrated qubits and the mode volume of the order of the wavelength cubed. Photonic crystal cavities can theoretically have a mode volume of less than 10^{-3} wavelengths cubed [106, 107] (Fig. 4d), but coupling of qubits to such cavities has not been demonstrated yet.

An important parameter of the qubit–cavity system is the *cooperativity*, which takes the spectral broadening of the optical qubit transition into account:

$$C = \frac{4g^2}{\kappa\gamma}\,, \tag{5}$$

where $g \propto 1/\sqrt{V}$ is the Rabi frequency for a single photon, and $\kappa \propto 1/Q$ and γ are the spectral widths of the cavity and of the optical transition in the qubit (with the different types of broadening taken into account). For $C \gg 1$, the qubit interacts with a single photon coherently, and maintaining high-efficiency logical operations between them becomes possible [110]. This regime has been achieved with neutral atoms ($C \geqslant 100$ [95]), color centers in diamond ($C \geqslant 100$ [55]), quantum dots ($C \geqslant 100$ [111]), and ions ($C \approx 10$ [112, 113]).

A large number of solid-state qubits exists [114–116], and we briefly discuss the most promising of them in Sections 3.2–3.6.

3.2 Nitrogen vacancy centers in diamond

A nitrogen–vacancy (NV) color center in diamond is formed by a nitrogen atom replacing a carbon atom and by a vacancy at a nearby lattice site (Fig. 5a). The optical transition at a wavelength of ~ 637 nm occurs between the electron energy levels located in the band gap of diamond, and quantum memory is based on the electron and nuclear spins. After the detection of a single NV center in 1997 [117], they have become a foundation for many breakthrough experiments in quantum optics [118] and magnetometry [119]. Over the last decades, a large amount of work has been done to create a

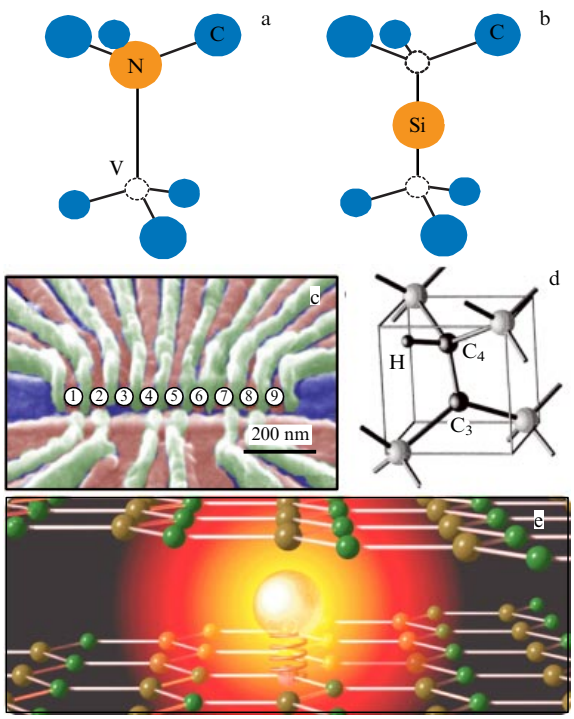

Figure 5. (Color online.) Examples of solid-state qubits. (a) NV centers in diamond. Blue dots: carbon atoms (C); white dot: vacancy (V) in the crystal lattice; N: impurity nitrogen atom substituting one C atom. (b) SiV center in diamond; impurity silicon atom (Si) is interstitial, ensuring a higher degree of symmetry than NV centers do. (c) Array of gate-defined QDs in silicon (reproduced from [128], published under the Creative Commons Attribution 4.0 International license). (d) Structure of the T-center in silicon. Two carbon atoms (C_3, C_4) substitute one silicon atom, and the hydrogen atom is bound to C_4 (reproduced from [129] with permission from the American Physical Society, © 1996). (e) Impurity atom located between two layers of hexagonal boron nitride (hBN) [130] (reproduced from [131] with permission from the American Physical Society, © 2020).

quantum node based on an NV center. For example, quantum memory with a coherence time longer than 1 s and a register of 10 qubits based on nuclear spins with two-qubit operations has been demonstrated [120, 121]. In addition, quantum entanglement of spatially separated qubits and entanglement distillation have been realized [72, 122]. Thus, NV centers satisfy all the above criteria except 4–6: they weakly interact with light.

Attempts to place NV centers into nanocavities led to a significant inhomogeneous broadening of the optical transition (γ in Eqn (5)) [123], which so far has prevented achieving the $C > 1$ regime required for effective interaction with photons. The main problem is the linear Stark effect and electrical noise in the nanocavity material. The linear susceptibility of NV centers to an electric field is explained by the presence of a nonzero static dipole electric moment ($\sim$ 1 D) due to the different electronegativities of nitrogen and the vacancies [124] (see Fig. 5), which cannot be eliminated. Although the nature of electrical noise is not fully understood, it is most likely caused by a change in the charge state of crystal lattice defects upon laser radiation required to control the NV center. These noises can be minimized by more gentle nanofabrication [125], but the prospects of using NV centers for quantum repeaters are still vague [126].

An alternative approach is based on the transformation of a telecommunication photon into mechanical vibrations (using optomechanical cavities), which can then interact with the electron spin of the NV center either directly [40, 80] or via magnetic field modulation [127]. In the future, this will allow circumventing the problem of electrical noise and creating an interface between an NV center and a photon operating at room temperature.

3.3 Silicon vacancy centers in diamond

A silicon–vacancy (SiV) color center in diamond consists of two vacancies in neighboring sites of the crystal lattice and a silicon atom between them (Fig. 5b). As in the case of NV centers, an optical transition at a wavelength of $\sim$ 737 nm occurs between the electron energy levels located in the band gap of diamond, and quantum memory is based on the electron and nuclear spins. SiV centers were discovered at the Lebedev Physical Institute (FIAN) in 1980 [132–134] and for a long time were considered an undesirable impurity in diamond, serving as an indicator of the artificial origin of diamonds. Everything changed in 2006, when SiV centers were discovered to be sources of single photons [135]. Two solid-state qubits were first entangled in a single nanostructure (nanowaveguide) in 2016 [136]. The first solid-state two-qubit quantum node with a deterministic interaction with photons and with a quantum coherence time greater than 1 ms was first built in 2019 [137, 138]. It thus follows that SiV centers satisfy all the criteria. Moreover, the quantum node has a bandwidth of more than 10 GHz due to the short lifetime of the excited level in nanocavities. Based on such a node, the first repeater that overcame the direct transmission limit was demonstrated in 2020 (see Section 4.1.2).

Thermally excited acoustic phonons in diamond at a temperature of 4 K have a frequency of about 100 GHz, which coincides with the value of the fine-structure splitting of the ground state of SiV centers (50–200 GHz). The resonance scattering of photons limits the coherence of SiV centers at a temperature of 4 K by a time of the order of 100 ns [139]. Achieving a coherence time longer than 1 ms would require cooling to temperatures of $\sim$ 100 – 500 mK [139, 140], which entails expensive dilution refrigerators and limits scalability.

The main reason for the success of SiV centers is their high symmetry, namely, the presence of an inversion center [141] (see Fig. 5), which guarantees the absence of a static electric moment; hence, SiV centers experience only the quadratic Stark effect. This leads to a slight broadening of the optical transition in nanocavities (by several natural widths) [142], allowing the regime with $C \geqslant 100$ to be reached [55]. The understanding of this fact was an impetus for studies of other color centers that have an inversion center [141] or a nearly zero difference between the dipole moments of the optical transition levels [124]. For example, color centers in diamond based on other impurity atoms of groups III [143] and IV (GeV [134, 144, 145], SnV [146, 147], and PbV [148]) also have the inversion symmetry and can operate at higher temperatures, close to 4 K, but their study is at an early stage.

3.4 Broadband semiconductors

The presence of a large number of color centers in diamond is due to a large band gap ($\sim$ 5.5 eV), as a result of which color centers emitting in the optical and near-infrared ranges are photostable. Of course, there are various other wide-gap semiconductors.

Hexagonal boron nitride. This material has a band gap of $\sim$ 6 eV and contains many color centers, which are now being

actively studied [149–152]. One color center deserves a separate discussion. In contrast to the spectral width of all other known color centers, its spectral width is practically independent of temperature: at a temperature of 300 K, a Fourier-limited line with a width of about 60 MHz is observed [130, 131]. For comparison, the typical spectral width of the remaining color centers is of the order of several nanometers. Although the nature of this defect is still poorly understood, as is its structure, the impurity atom is believed to be located between the hBN layers (Fig. 5e) and interacts weakly with phonons [130, 131]. It is not known whether this center has the electron spin required for quantum memory, but it can be used to create a source of single photons with a Fourier-limited spectral width even at room temperature.

Silicon carbide. This semiconductor has a band gap equal to 2.3–3.3 eV, depending on the polytype. Although the crystal structure of SiC does not allow color centers to have an inversion center, whose importance was mentioned above, one center, silicon–vacancy, does have similar static electric moments in the ground and excited energy levels [124], which ensures its efficient integration into optical nanocavities.

Also very promising are several color centers that have a quantum memory with a coherence time longer than 1 ms at a temperature of 4 K and emit in the telecommunication range [153, 154], making the wavelength conversion unnecessary.

3.5 T-centers in silicon

The nanofabrication processes of the semiconductors listed above are very complex, which limits their prospects and increases the production cost. The most technologically advanced material is silicon, for which methods of purification and nanofabrication have been developed in the global semiconductor industry. It would therefore be very convenient to construct quantum networks based on color centers in silicon; but because of the small band gap (1.14 eV), most color centers emitting in the telecommunication range are photo-unstable due to two-photon ionization. However, recent results with T-centers (discovered back in 1996 [129]) indicate their photostability [155, 156]. The long coherence time of quantum memory ($\sim$ 1 ms for electron spin and $\sim$ 1 s for nuclear spin) and the 1.326-nm wavelength falling into the telecommunication domain [155, 156] make T-centers a promising candidate for the creation of quantum nodes.

3.6 Quantum dots

Quantum dots (QDs) are semiconductor devices in which the motion of charge carriers is quantized in all three spatial directions (0-dimensional systems) [157]. We briefly consider two types of QDs that are of interest for quantum networks.

Epitaxial (self-assembled) QDs are nanoscale heterostructures ($\sim$ 10 nm). In them, due to the combination of semiconductors with different bandgap widths, charge carriers can be spatially localized, and the small size of these QDs gives rise to discrete energy levels [158]. The qubit is realized as the spin of an electron captured by the QD, and the emission of a photon is effected by exciting the electron, which then transfers to the conduction band, and the resulting exciton (electron–hole pair) then undergoes radiative recombination [159]. Such QDs, after being placed in nanocavities, demonstrate excellent optical properties and can have a single-photon cooperativity $C > 100$ [111, 158]. On the other hand, suitable direct-gap semiconductors (e.g., GaAs) do not have spinless isotopes. Magnetic dipole–dipole interaction between their nuclear spins and the spin of a captured electron leads to the decoherence of the latter and limits the quantum memory time to several microseconds [160]. This coherence time is too low for a multifunctional quantum node, but it is suitable for some quantum repeater protocols (see Section 4.2) or for creating a single-photon source.

Another class comprises *electron* (*gate-defined*) QDs, in which a two-dimensional electron gas that forms near the semiconductor surface is captured into electrostatic traps created by deposited electrodes [161]. Factors such as a long-term quantum memory (longer than 20 ms [162]) due to the use of materials with spinless isotopes, the deterministic creation of QD arrays, and the possibility of performing quantum operations between them [163] make such QDs viable candidates for use in quantum computers [164]. However, electron QDs are not optically active, which complicates their use in quantum nodes.

An interesting and promising avenue is the creation of QDs in two-dimensional semiconductors with a thickness of one or two atomic layers [165]. For example, transition-metal dichalcogenides [166] have a direct band gap and a high exciton binding energy [167, 168], and can be made of spinless isotopes. This provides hope for the creation of QDs that would simultaneously be optically active [169, 170] and have a long-term quantum memory, which is necessary for constructing a quantum node.

4. Quantum repeaters

Quantum repeaters are a special case of quantum network nodes. The tasks of a quantum repeater are similar to those of a classical optical fiber amplifier: to 'compensate' for light scattering in an optical fiber and to maintain the exchange of quantum information between remote network nodes [21], replacing the exponential dependence in (1) with a polynomial one.

4.1 BDCZ protocol

We briefly consider the first quantum repeater protocol (BDCZ) proposed in 1998. We assume that a communication channel of the length L between Alice and Bob is divided into $N+1$ equal-length segments, and we place there N additional nodes — quantum repeaters, each of which has two qubits L_i and R_i that can store quantum information for a long time (Fig. 6). We then bring the qubits R_i and L_{i+1} of adjacent nodes into the maximum entangled state [72, 171] using a quantum communication channel between them (for example, by sharing the EPR (Einstein–Podolsky–Rosen) photon pair between them). Then, we create entanglement between qubits A and L_1 and between B and R_N. Due to losses in the optical fiber, the generation of a delocalized entangled state is a random process, and if quantum repeaters had not had long-term quantum memory, the total probability of *synchronous* pairwise entanglement of all adjacent nodes would still have been given by $\exp(-\alpha L/10)$. But quantum memory allows this process to be implemented *asynchronously*, thereby eliminating the exponential dependence on distance.

The next step is the entanglement swapping [65, 66]. For example, if node k measures two of its qubits in the Bell-state basis [172], then qubits R_{k-1} and L_{k+1} become entangled. After repeating this process with all N nodes, Alice's and Bob's qubits become entangled; the desired goal is achieved. An illustrative example of how asynchronicity works is discussed in Section 4.1.1.

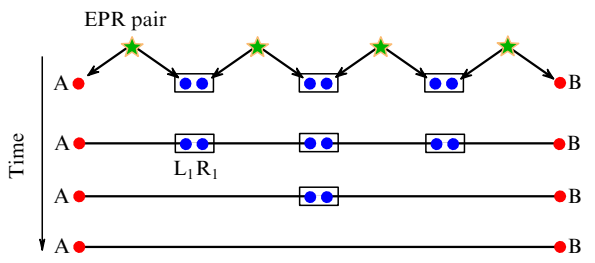

Figure 6. (Color online.) Diagram of the quantum repeater operation. The task is to entangle two qubits held by Alice (A) and Bob (B). Placed between them are quantum repeaters (black rectangles), each containing two qubits, L and R (blue dots). The source of EPR pairs (stars) distributes the entangled photons to the neighboring nodes.

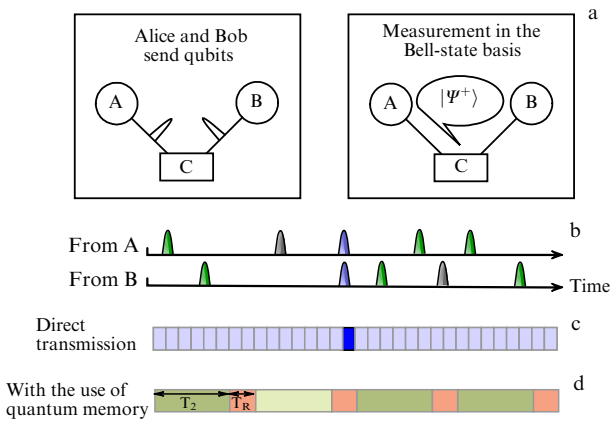

Figure 7. (Color online.) Advantages of using quantum memory [55]. (a) MDI-QKD scheme: Alice (A) and Bob (B) send photons to Charlie (C), who measures them in the Bell-state basis. (b) Photons that have reached Charlie. (c) In the absence of quantum memory, Charlie can measure only when both photons from Alice and Bob arrive to him simultaneously (blue rectangle). (d) Quantum memory allows Charlie to perform measurements asynchronously (dark green rectangles), which increases the success probability. (Reproduced from [55] with permission from Springer Nature, © 2000.)

Of course, this reasoning does not take many of the physical limitations of existing systems into account. For example, partial decoherence of an EPR pair during propagation in an optical fiber and a finite error probability of local quantum operations on quantum-repeater qubits lead to the 'nonideality' of the entangled state $|\Psi\rangle$ between adjacent nodes. If the *fidelity* of this state is $\langle\Psi|\Psi_0\rangle = 1 - v$, where $|\Psi_0\rangle$ is one of the maximum-entangled two-qubit (Bell) states, then the fidelity of the final entangled state between Alice and Bob can be estimated as $P = 1 - Nv \approx \exp(-Nv)$, which gives an exponential decrease as the number of quantum repeaters increases. If $P < 85\%$, then this state can no longer be used for QKD [16].

To improve the precision of the entangled state, *entanglement distillation* has to be used [85, 173, 174], which consists of using several copies of entangled states to create one entangled state with improved characteristics. The probability of errors in local quantum operations can also be reduced by *quantum error correction algorithms* [175, 176]. All these steps result in an increase in the required resources (the number of qubits), complicate the creation of a quantum network, and reduce its operation speed. The number of required resources and error correction protocols are considered in more detail in [177, 178].

Effective implementation of the quantum repeater protocol is hampered by the lack of a physical qubit platform that would satisfy all the criteria listed in Section 3. Nevertheless, a huge amount of work has been done over the past two decades: prototypes of quantum nodes have been created based on atomic ensembles [71, 179–181] (using a modified protocol [22, 182, 183]), color centers [72, 120, 121, 137], superconducting qubits [10, 82, 184, 185], ions [186–189], and neutral atoms [102]. Unfortunately, most of these systems cannot increase the communication channel bandwidth, which is the purpose of a quantum repeater. The reason for this is the short-lived quantum memory, the absence of an efficient interface with optical photons, and the finite fidelity of local quantum operations (see Section 4.1.2).

4.1.1 Asynchronicity. For a clear demonstration of exactly how quantum memory helps increase the throughput of a quantum network, we consider a modification of the BB84 QKD protocol, a measurement-device-independent QKD (MDI-QKD) [16, 190]. For this, Alice and Bob each send a single photon to Charlie, who is located between them, at the distance $L/2$ from each of them (Fig. 7). Charlie measures the photons received from Alice and Bob in the Bell-state basis $(\{(|00\rangle \pm |11\rangle)/\sqrt{2}, (|01\rangle \pm |10\rangle)/\sqrt{2}\}$, where $|0\rangle$ and $|1\rangle$ are the quantum states of the sent photons); Charlie then publicly announces the measurement results. This measurement only tells whether Alice and Bob transmitted the same bits, but does not reveal the values of the bits. This is sufficient for Alice and Bob to generate a shared encryption key, but this information is insufficient for an attacker. Obviously, if Charlie has no quantum memory, then the photons from Alice and Bob must reach Charlie synchronously for the measurement to be successful. Because the probability that a photon from Alice or Bob reaches Charlie is equal to $\sqrt{p_0}$, the probability of success (that both photons reach Charlie at the same time) is still $\sqrt{p_0}\sqrt{p_0} = p_0$, Eqn (1).

This scheme has two major advantages over BB84. First, the degree of secrecy can easily be determined by checking the violation of Bell's inequalities, even if an attacker controls Charlie's equipment. Second, because the communication channel contains two photons (per bit of information) simultaneously, the signal-to-noise ratio during detection is higher, allowing a higher encryption key generation rate [190].

We now let Charlie operate a simple quantum computer consisting of two qubits C_l and C_r, with a coherence time T_2, capable of writing the states of single photons to these qubits. We consider the following protocol.

(1) Alice and Bob each send Charlie a single photon at a rate f.

(2) If Charlie receives a photon from Alice (Bob), he writes its quantum state into his qubit C_l (C_r) and ignores all subsequent photons from Alice (Bob).

(3) Steps 1 and 2 are repeated until Charlie receives both photons. If this does not happen within time T_2, then everything is repeated from the start.

(4) Using local operations on his quantum computer, Charlie then measures C_l and C_r qubits in the Bell-state basis.

During time T_2, Alice and Bob send $n = fT_2$ photons each. If quantum memory is not used and if $np_0 \ll 1$, then, during time T_2, both photons simultaneously reach Charlie at least once with probability np_0 or, in the general case,

$$p_{\mathrm{DT}} = 1 - (1 - p_0)^n \approx np_0 \,. \tag{6}$$

But if quantum memory is used, it suffices that the photons reach Charlie asynchronously during time T_2. The probability of a photon from Alice or Bob reaching Charlie in n tries is $n\sqrt{p_0}$. Because the photons from Alice and Bob can now be registered asynchronously, the total probability of success is $n^2 p_0$ or, in the general case,

$$p_{\mathrm{QR}} = \left(1 - (1 - \sqrt{p_0})^n\right)^2 \approx n^2 p_0 \,. \tag{7}$$

We see that quantum memory gives a gain proportional to n, the number of tries it takes to send a photon within the quantum memory coherence time. A more precise comparison requires finding the capacity of the channel in each case. For the considered MDI-QKD method, the channel capacity is the number of bits of a secret key that can be received if one *pair* of photons is sent. For the repeater-free method, we obviously have

$$r_{\mathrm{DT}} = \max\left(\frac{p_{\mathrm{DT}}}{n}\right) \approx p_0 \,, \tag{8}$$

which naturally coincides with the direct transmission limit in (2) (see Section 2). With a quantum repeater in use,

$$r_{\mathrm{QR}} = \max\left(\frac{p_{\mathrm{QR}}}{n}\right) \approx \sqrt{p_0} \,, \tag{9}$$

which attains a maximum at

$$T_2^{\mathrm{opt}} \propto \frac{1}{\sqrt{p_0}} \,. \tag{10}$$

This means that a quantum repeater can indeed give an essential gain in the quantum network operation speed (Fig. 8).

4.1.2 Direct transmission limit. A major difficulty in demonstrating a quantum repeater that could increase the throughput of a quantum communication channel in comparison with the direct transmission limit is the need to create a quantum node having two properties simultaneously: (a) a long quantum memory time T_2 and (b) a high fidelity of quantum operations. The necessity of condition (a) follows from Eqn (10).

Figure 8 shows how the finite time of quantum memory affects the performance of a quantum repeater. Because of infidelities in quantum operations, Alice and Bob detect errors in the received encryption key. Such errors can be caused not only by the infidelities of quantum operations but also by the actions of an attacker, and therefore Alice and Bob need to *distill* the encryption key to ensure its secrecy [16]. But, as a result of this, the final encryption key contains only $1 - \mathrm{QBER}/15\%$ of bits of the original key, where QBER (quantum bit error rate) is the total error probability. For example, with $\mathrm{QBER} \approx 14\%$, only 7% of bits can be used (see Fig. 8), and if $\mathrm{QBER} > 15\%$, the encryption key cannot be created.

Only recently has it become possible to resolve these difficulties and overcome the direct transmission limit by using a quantum node consisting of an SiV center in diamond [137] placed into a photonic crystal cavity (Fig. 9). Simple QKD scheme demonstrated in Ref. [55] is four times faster than the direct transmission of a photon after distillation, and 80 times faster than the transmission without distillation (see Fig. 9). The different slopes of the red and green lines in Fig. 9c

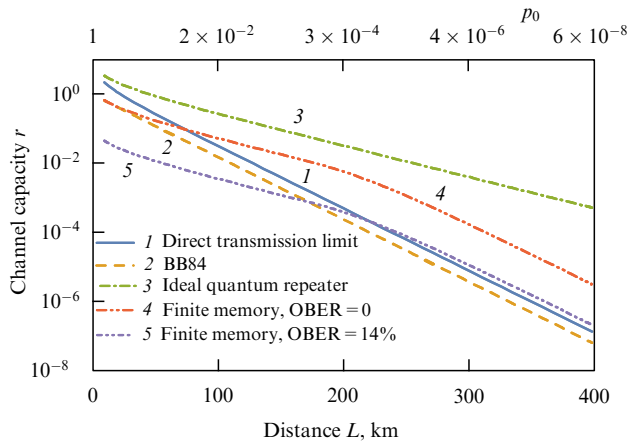

Figure 8. (Color online.) Quantum channel capacity for QKD at the distance L of the optical fiber with a loss of 0.18 dB km^{-1} and an ideal photodetector (quantum efficiency 100%, zero dark current). *1* — direct transfer limit; *2* — ideal BB84 protocol; *3* — ideal quantum repeater; *4* — quantum repeater discussed in Section 4.1, with $n = 50$; *5* — quantum repeater with $n = 50$ and QBER = 14%.

reflect the gain due to the change of the linear dependence on p_0 with the square-root dependence (see Eqns (2) and (4)).

Moreover, the obtained $\mathrm{QBER} < 11\%$ provides the security of the generated secret key to any types of attacks [16]. This was achieved because of the high cooperativity $C > 100$, the long-term quantum memory (> 100 μs), and the possibility of measuring the SiV-center state with a fidelity $F > 0.99$. In this experiment, the effective loss between Alice and Bob was 80 dB, which corresponds to $L = 400$ km of optical fiber at a wavelength of 1550 nm. We note that SiV centers emit photons at a wavelength of 737 nm and must first be converted into the telecommunication band (see Section 5).

4.2 One-way quantum repeaters

The quantum repeaters discussed above have a number of significant disadvantages. Because the generation of entanglement between neighboring nodes occurs at random instants, such nodes require qubits with long-term quantum memory. This also leads to the need for a two-way exchange of classical information between nodes to confirm the success of each operation (two-way signaling). All this limits the speed of the quantum network [89, 177]. To eliminate these disadvantages, schemes have been developed, called *one-way quantum repeaters*, in which information propagates sequentially along the entire chain of quantum repeaters, resembling classical computer networks [86, 193–196]. In these schemes, neighboring nodes are not entangled in advance, in contrast to those of a conventional quantum repeater [21], and quantum information is not transferred between nodes by single photons but by special multiphoton entangled states, *tree cluster states* [192, 197]. Due to their special structure, such states make it possible to successfully transmit quantum information encoded in them even in the case of significant losses in the optical fiber; for example, the state shown in Fig. 10 is stable at losses up to 50% [192] (about 15 km of optical fiber).

The protocol works as follows [86].

(1) Alice creates a tree cluster state such that the root node is a stationary qubit and all other qubits (leaves) are photons.

(2) Alice then *encodes* the state of her qubit (A) into a cluster state by jointly measuring A and the root of the cluster

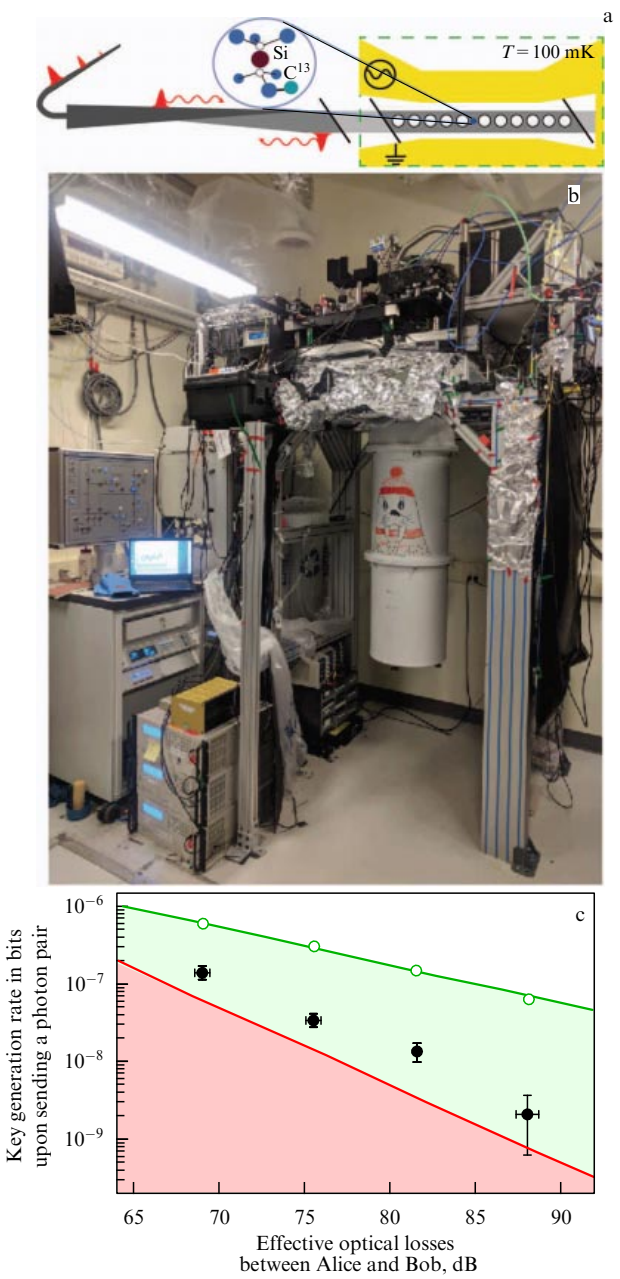

Figure 9. (Color online.) Overcoming the direct transmission limit. (a) Setup of a quantum node: an SiV-center is located in the center of a photonic crystal cavity (gray rectangle), a gold microwave waveguide (yellow) is sputtered on it, and the photonic cavity is adiabatically coupled to a single-mode optical fiber (left) (reproduced from [191] with permission from the American Physical Society, © 2019). (b) Photo of the experimental setup: a dilution refrigerator is in the center, with a diamond sample placed inside it. (c) Rate at which the secure key is generated depending on effective optical loss between Alice and Bob. Red line: theoretical limit for the direct transmission MDI-QKD, Eqn (2). Green circles: sifted key rate with the use of quantum memory. Black dots: key generation rate after error correction (reproduced from [55] with permission from Springer Nature, © 2020).

state in the Bell-state basis. Because the root qubit is entangled with the rest of the leaves, this actually implements a *quantum teleportation* of the A qubit to the remainder of the cluster state.

(3) The cluster state no longer contains a stationary root and is sent toward the first repeater.

(4) The quantum repeater measures the photons in the received cluster state at levels 2 and 3, thereby determining which of the level-1 (L_1) photons was not lost in transmission. After measuring the photons of levels 2 and 3, the L_1 photon contains the information encoded by Alice [192].

(5) The quantum repeater creates its own cluster state with a stationary root qubit.

(6) The quantum repeater then teleports the chosen L_1 photon to its cluster state (*transcoding*) and sends it further.

(7) Finally, Bob determines the surviving level-1 photon of the received cluster state and writes it to his stationary qubit.

This system can be used as follows: Alice creates an entangled state of two qubits, stores one qubit for herself, and encodes the other into a cluster state, which she sends through a chain of quantum repeaters to Bob, who stores the received qubit into his memory. As a result, Alice and Bob share a pair of entangled qubits. Cluster states can also be used in the BDCZ protocol to speed up the entanglement generation between neighboring nodes in a network.

The simplest implementation of this method requires one qubit with an efficient photonic interface and two additional logical qubits [86]. (Error correction and entanglement distillation, naturally, lead to a larger number of qubits.) In this case, information must be stored only until the received cluster is measured and a new cluster is created, which can be done rather quickly (in $\leqslant 1$ μs), whereas, in the case of a conventional quantum repeater, the coherence time must be no less than the time spent by a photon on the path between neighboring nodes (100 μs corresponds to about 100 km).

Currently, the deterministic generation of a simple cluster state is being demonstrated using QDs [198, 199]. Also, the efficient photonic interface, long-term quantum memory, and interaction with nuclear spins demonstrated recently make silicon vacancies in diamond a possible candidate for the creation of such quantum repeaters in the foreseeable future [55, 137, 140].

4.3 All-photonic quantum repeaters

Photonic cluster states can be used not only for the transmission of quantum information through a lossy channel but also for measurement-based quantum computing [197, 200, 201]. In 2015, the scheme of an *all-photonic quantum repeater* was proposed where photonic cluster states are used to store, process, and transfer qubits [202]. Such a quantum repeater does not in principle require any quantum memory based on atoms or solid-state systems, which are the main difficulties in creating the quantum repeaters considered in Section 4.2. However, the deterministic creation of a nontrivial photonic cluster state is possible only with the use of a single-photon source with quantum memory [198, 199, 203, 204], which appears to make such schemes comparable in complexity to the preceding ones. Nevertheless, the first demonstrations of a prototype quantum repeater without stationary qubits using spontaneous parametric down conversion for the probabilistic generation of cluster states [59, 205] were carried out in [206, 207].

5. Wavelength conversion

Optical-fiber losses are highly dependent on the wavelength of light (Fig. 11). Existing quartz optical fibers have the lowest losses at wavelengths of 1300 and 1550 nm, and therefore the range of quantum networks can be increased by using photons whose wavelength falls into these *telecommunication bands*. However, most qubits emit at shorter wavelengths and

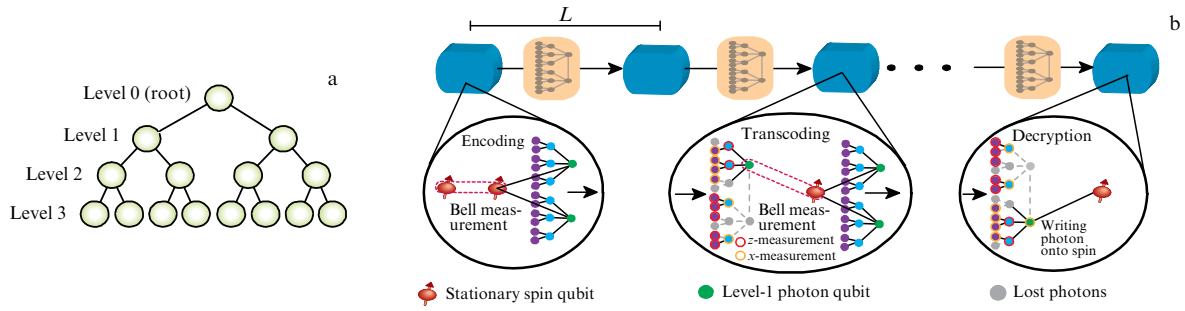

Figure 10. (Color online.) One-way quantum repeaters. (a) Example of a tree-like cluster state. Circles (vertices of the graph) are qubits, edges connect pairwise entangled qubits (reproduced from [192] with permission from the American Physical Society, © 2006). (b) Diagram of a repeater based on cluster states (reproduced from [86], published under the Creative Commons Attribution 4.0 International license).

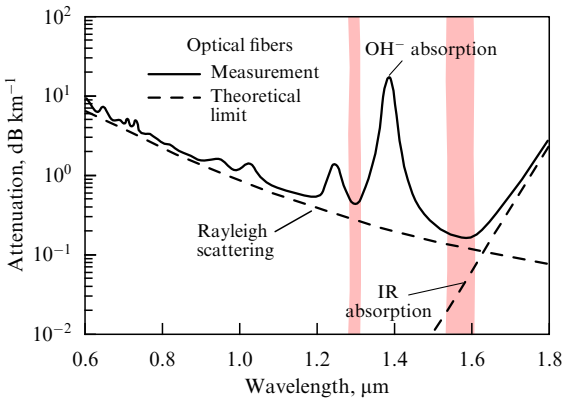

Figure 11. Wavelength dependence of losses in a quartz optical fiber. Colored strips show the principal telecommunication bands corresponding to minimal losses (≈ 1300 and 1550 nm). (Courtesy of E F Schubert.)

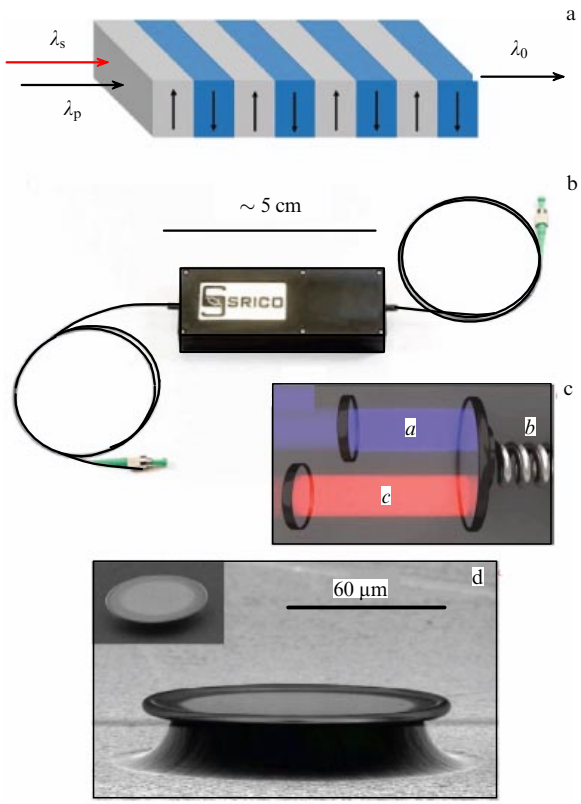

Figure 12. (Color online.) Wavelength converters. (a) Periodically poled nonlinear optical crystal. Arrows indicate direction of polarization. (b) Integrated periodically poled crystal ready for connection to an optical fiber network (reproduced with permission from © Srico Inc.). (c) Schematic representation of two optical modes of the resonator (a, c) interacting with a mechanical resonator (b) (reproduced from [208], published under the Creative Commons Attribution 4.0 international license). (d) Example of an optomechanical resonator, a microdisk (reproduced from [209] with permission from Springer Nature, © 2003).

require an additional conversion. Such converters must have the following properties:

(1) high quantum efficiency;

(2) preservation of coherence;

(3) low additional noise.

The last two items are the most important ones, because even a 10% efficiency in converting wavelengths from 740 nm to 1300 nm increases the distance that a photon can be sent from 10 to 100 km. Coherence is required to maintain quantum entanglement, for example, between a photon and an atom that emitted it. Low additional noise is necessary, in particular, to maintain the single-photon nature of the radiation. Moreover, the signal-to-noise ratio (SNR) sets a lower bound on the error probability in each individual bit of the encryption key for QKD as $\mathrm{QBER} \geqslant 0.5\,\mathrm{SNR}^{-1}$, because the detecting device cannot distinguish a 'good' photon from a 'bad' one, leading to an incorrect result with a 50% probability. When $\mathrm{QBER} > 15\%$, the key cannot be used for encoding [16]; hence, a criterion for the practicality of a wavelength converter for the simplest BB84 protocol can be formulated as $\mathrm{SNR} \geqslant 3.5$. Currently, there are two main approaches to wavelength conversion: nonlinear optics and optomechanics.

The *nonlinear optical method* typically involves a stimulated parametric conversion of the light frequency [210–212], with the original photon (with wavelength λ_s) mixed with the pump laser photon (λ_p), which leads to the generation of a photon at the difference frequency ($\lambda_0^{-1} = |\lambda_s^{-1} - \lambda_p^{-1}|$). Like all nonlinear processes, parametric generation requires a high intensity of the pump laser light to obtain a high conversion efficiency [213], which can be achieved using optical cavities [214]. However, such cavities require careful alignment and active length stabilization, which makes them somewhat impractical for a widespread use outside physics laboratories.

More practical is the use of waveguides made of periodically poled nonlinear crystals, in which the direction of one of the principal birefringence axes changes periodically by 180° [215] (Fig. 12). First, the periodic structure allows using quasi-phase matching to choose the orientation of the

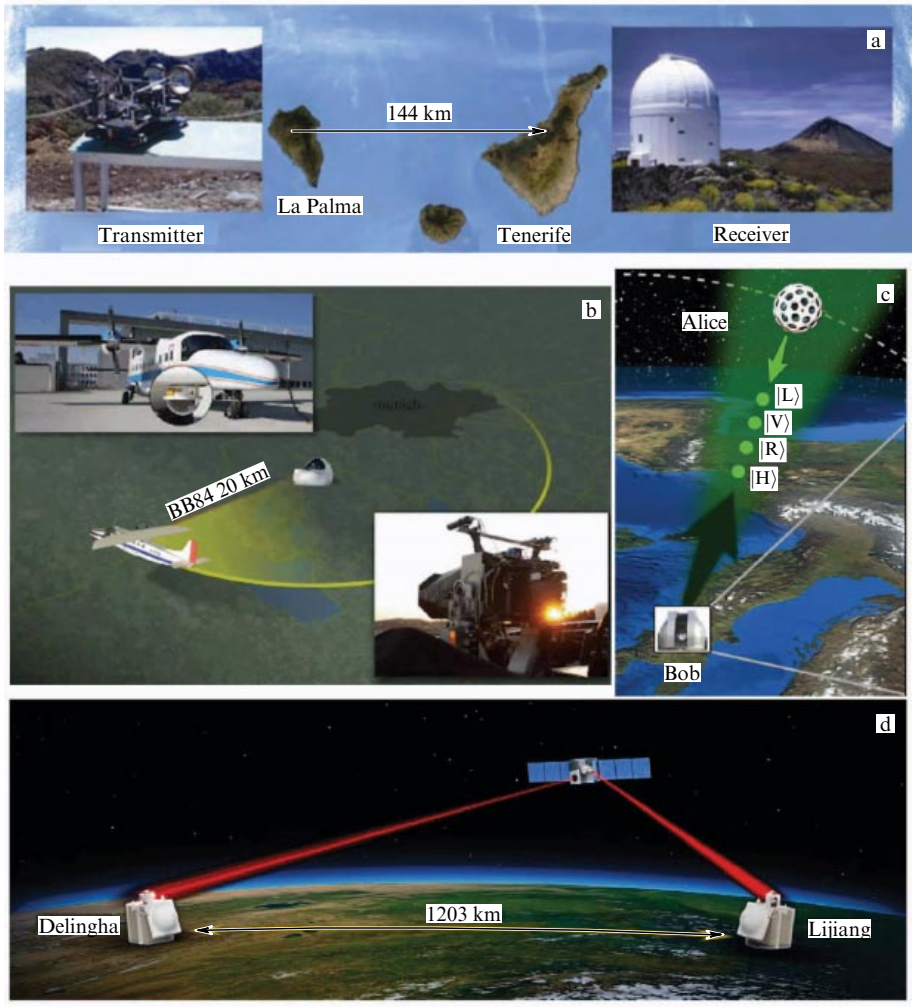

Figure 13. (Color online.) Atmospheric quantum cryptography. (a) QKD between two Canary Islands. Transmitting device is shown on the left, receiving telescope, on the right (reproduced from [223] with permission from Springer Nature, © 2007). (b) QKD between ground station and an aircraft (reproduced from [224] with the permission of the authors, H Weinfurter and F Moll, and the publishing house Society of Photo-optical Instrumentation Engineers (SPIE), © 2012). (c) QKD using a satellite as a retroreflector (reproduced from [225] with permission from the American Physical Society, © 2015). (d) Depiction of the distribution of quantum entanglement using a source of entangled photons located on a satellite [226].

crystal at which spatial drift of radiation is zero [216], and, second, the small cross section of the waveguide increases the light intensity. This makes it possible to use waveguides made of crystals, such as lithium niobate (PPLN), several centimeters in length, which significantly increases the efficiency of the wavelength conversion of light without the use of cavities.

One of the difficulties in parametric generation is related to the low SNR ratio due to noise photons caused by inelastic scattering of the high-power pump laser. The wavelength of a scattered photon is almost always greater than the original wavelength, and, therefore, if $\lambda_p > \lambda_0$, then the scattered photons can be easily filtered out by spectral methods. For example, in [217], the conversion of QD radiation from $\lambda_s = 711$ nm to $\lambda_0 = 1313$ nm was demonstrated using a pump laser with $\lambda_p = 1550$ nm, which allowed obtaining SNR ≈ 50. In contrast, conversion of radiation from NV centers (640 nm) to the telecommunication band ≈ 1300–1500 nm requires pumping at a shorter wavelength, which complicates obtaining a high SNR [218].

It is also possible to use the sum-frequency generation $\lambda_0^{-1} = \lambda_s^{-1} + \lambda_p^{-1}$. This allows converting a photon from the telecommunication to the optical band, which is beneficial for the BDCZ repeater scheme, where neighboring network nodes are entangled by splitting an EPR photon pair (see Fig. 6). Such a pair can initially be generated in the telecommunication band and then frequency-converted in a quantum repeater. For example, to convert from $\lambda_s = 1310$ nm to $\lambda_0 = 737$ nm (the emission wavelength of an SiV center in diamond), a pump laser at wavelength $\lambda_p = 1700$ nm is used. Because $\lambda_p \gg \lambda_0, \lambda_s$, the pump laser introduces practically no noise. But, if $\lambda_p < \lambda_s$, the spectrum of noise photons from the scattering of pump laser photons overlaps with the spectrum of the original photon λ_s, leading to a decrease in both the SNR and the coherence of the transformation. Nonlinear converters based on PPLN are already available commercially in integrated form (see Fig. 12) and can easily be integrated into optical-fiber networks with a loss < 4 dB.

The *optomechanical method* is based on coupling two optical modes via mechanical vibrations of a resonator [219–221]. This approach is still much inferior to nonlinear optics in terms of efficiency, but it has a number of significant advantages. First, due to their small size (≈ 100 μm), such microcavities can be integrated on a chip and mass-produced. Second, this method is capable of not only converting light from the optical to the infrared band, but also converting microwave photons into infrared light, which is needed for

connecting superconducting quantum computers to quantum networks [87, 88]. A disadvantage is the need to cool microcavities to cryogenic temperatures to suppress thermal noise, but most qubits already require temperatures < 4 K.

An interesting application of optomechanical cavities is the creation of an interface between telecommunication photons and qubits without using an optical transition in a qubit. For example, this would allow superconducting quantum computers to be connected to quantum networks by converting microwave photons into infrared ones [87, 88]. Moreover, the spin degree of freedom of most solid-state qubits discussed in Section 3 can be controlled using phonons, and therefore optomechanical cavities can be used to couple such qubits with telecommunication photons even in the case of a weak or unstable optical transition in a qubit (for example, in NV centers) [127].

6. Repeater-free methods

As noted above, quantum repeaters will allow deploying a global quantum network, but their creation is a very complicated technological task. However, there are several trade-off solutions. In Section 6.1, we discuss the use of satellites to distribute entangled photons between two remote users on Earth. In Section 6.2, we describe a hybrid approach for QKD involving *trusted nodes*, and in Section 6.3, a revolutionary QKD scheme that overcomes the direct transmission limit and doubles the QKD range without using quantum memory [222].

6.1 Satellites

The absorption of light in an optical fiber limits the practical range of quantum cryptography and the scale of quantum networks without quantum repeaters to a distance of about 100 km. In the atmosphere, scattering can be less than in an optical fiber, which is why experiments on atmospheric QKD have been started [227], although the natural curvature of the Earth's surface sets a stringent limit on the line-of-sight distance: about 10 km for observers at sea level.

To implement QKD and distribute entanglement over a distance of about 100 km, the elevated transmitting and receiving devices were used [223, 228–231] (Fig. 13a). The use of satellites allows two users who are not in line of sight to be linked by a quantum channel [232]. The first experiments in this area consisted of the implementation of QKD between a ground station and an aircraft [233] (Fig. 13b) with a satellite used as a retroreflector [225] (Fig. 13c). The effective channel loss between the ground station and the satellite at an altitude of 1000 km can be as low as 40 dB, which is comparable to losses in a 200-km optical fiber [234].

In 2017, a source of entangled photons located on a satellite was used to distribute these photons between two ground-based laboratories separated by 1200 km [226] (effective losses 60–80 dB, which corresponds to ~ 400 km of optical fiber). In 2020, the first QKD via a satellite was demonstrated [235] (E91 protocol [236], secure key generation rate 0.12 bits per second). Because the violation of Bell's inequalities was observed in this case, such photons can also be used to test fundamental physical theories [237, 238].

Unlike portable satellite phones, which use a relatively high radio wave power, quantum cryptography requires single photons. Their effective detection and, accordingly, higher throughput of the quantum channel require astronomical telescopes which continuously monitors the position of the satellite (Fig. 13a). The high cost of satellites and telescopes is likely to prevent this technology from entering our everyday life.

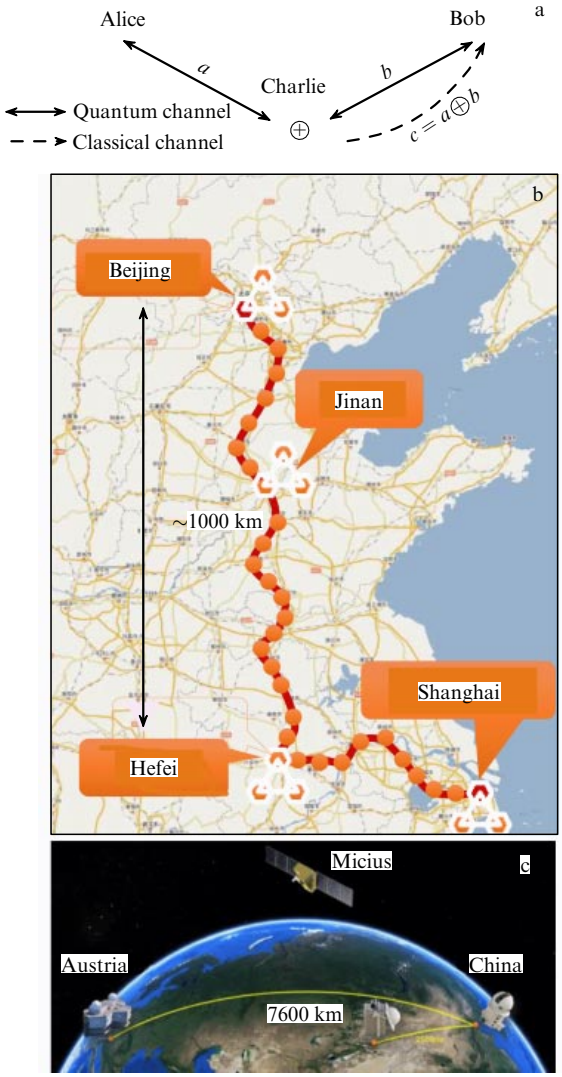

Figure 14. QKD with trusted nodes. (a) Principle of operation of a trusted node. (b) Quantum trusted node network in China between Beijing and Shanghai [239]. (c) QKD between China and Austria using the Micius satellite as a trusted node [239]. (Figures b and c are reproduced from [239] with permission from the Optical Society of America, © 2018, under the terms of the OSA Open Access Publishing Agreement.)

6.2 Trusted nodes

If a full-fledged quantum network capable of distributing entanglement between nodes is not needed and the task is to only increase the range of QKD systems, *trusted nodes* working like classical relays can be used (Fig. 14). The following example explains the essence of this method. Let Alice and Bob again want to generate a secret key, but the distance L between them is too long for the existing QKD systems to be used. We place Charlie, acting as a trusted node, in the middle between Alice and Bob. Let Alice and Charlie generate a key a, and Bob and Charlie in turn generate a key b using any QKD protocol. Charlie now generates a new key using bitwise 'exclusive or' ($\oplus$),

$$c = a \oplus b\,, \tag{11}$$

which he sends, for example, to Bob over a classical unprotected channel (in principle, it can be sent to all network participants). Bob computes Alice's key a using his private key b:

$$c \oplus b = a \oplus b \oplus b = a\,, \tag{12}$$

which Alice and Bob can then use to encrypt their messages.

Obviously, if an attacker intercepts key c, then, without knowing key b, which is known only to Bob and Charlie, the attacker is not able to determine a. Thus, if Charlie is isolated from the outside world (protected from eavesdropping), then the QKD using trusted nodes has the same degree of secrecy as the conventional QKD.

Thanks to this method, instead of generating a key at a distance L with a success probability p_0, two keys are generated at a distance $L/2$ with the success probability $\sim \sqrt{p_0}$. Recalling an example from Section 2, one such trusted node would reduce the time required to generate one bit of the secret key at distance $L = 1000$ km from 1 year to 1 s!

QKD networks based on trusted nodes have already been deployed in many countries and stretched for several thousand kilometers (in China [239], Japan [240], and England [241]). In Russia, the development and implementation of such networks are carried out by the Russian Quantum Center, Lomonosov Moscow State University, and other scientific institutions [242] with the support of the Russian Railways (RZD) [243]. Also worth mentioning is a recent experiment with a satellite used as a trusted node [244]. There, a secret key was generated at the rate of ~ 1 kbps between users in Austria and China separated by a distance of 7600 km. It was not required that both ground users be simultaneously in the line of sight with the satellite: secret keys are generated asynchronously and are stored on the satellite.

The main problem with this approach is to protect trusted hosts from eavesdropping, but the same problem exists for 'classic' QKD systems that store generated keys on ordinary computers, most likely connected to public data exchange networks and exposed to the risk of secret keys being stolen.

6.3 Twin-field quantum key distribution

In 2018, a revolutionary new method called the *twin-field QKD* was proposed. This method, similarly to a quantum repeater, overcomes the direct transmission limit and doubles the distance available for QKD without using quantum memory [222].

To explain this method, we consider the following experiment (Fig. 15). Let Alice and Bob each have a laser, and the lasers be phase-coherent with each other. Alice and Bob each prepare a weak laser pulse (with the average number of photons < 1) and send it to Charlie, located at the distance $L/2$ from them. In doing so, Alice (Bob) encodes the value of the sent bit $b_{\mathrm{A}}(b_{\mathrm{B}}) = 0$ or 1 in terms of the phase of her (his) laser pulse: $\phi_{\mathrm{A(B)}} = \pi b_{\mathrm{A(B)}}$. The photons interfere on a beam splitter, and, depending on the relative phase $\Delta\phi = \phi_{\mathrm{A}} - \phi_{\mathrm{B}}$ between these pulses, either detector D_0 fires (if $\Delta\phi = 0, 2\pi$) or detector D_1 does (if $\Delta\phi = \pi$), which is publicly reported by Charlie. Using information from Charlie, Alice and Bob can then see whether they have sent the same bits. In any case, they can agree on a secret key, but this information is not enough for an attacker to compromise the secret key.

The main feature of this method is that such interference persists even when only one laser pulse reaches Charlie. This is explained by the fact that a beam splitter erases information

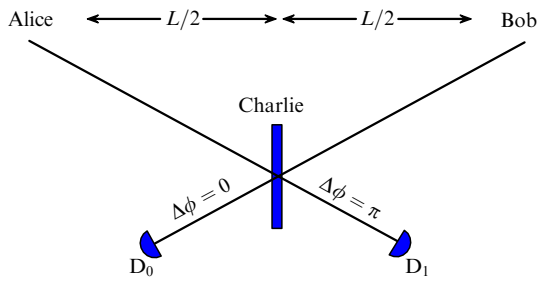

Figure 15. Scheme of a twin-field QKD.

about which side the arriving photon came from (whether from Alice or Bob) [245]. Thus, this method supersedes the *two-photon interference* used in the MDI-QKD scheme [190] with *single-photon interference* [246], and because only one photon is now required to reach Charlie, the dependence of the key generation rate on the distance becomes $r \propto \sqrt{p_0}$, just as with a quantum repeater.

The problem with the considered method — the need to stabilize the difference in the lengths of the interferometer arms (which can be more than 100 km) with an accuracy better than the wavelength of light ($\ll 1$ μm) — was not an obstruction to the first laboratory experiments [247, 248]. Later, another version of this method was proposed and implemented that does not require stabilizing the interferometer [249, 250], and in 2020 it became possible to experimentally implement a QKD that surpassed the direct transmission limit [251].

It is also worth noting that a similar single-photon interference was used in a recent experiment on the entanglement of two NV centers [72].

7. Conclusions

We live in an era when quantum technologies are entering our daily lives and the creation of a global quantum Internet will open up unprecedented horizons of new scientific and practical applications. The main obstruction is the absorption and scattering of photons, which impose restrictions on the distance that can be covered by a quantum network.

In this review, we discussed different approaches to solve this problem — quantum repeaters, trusted nodes, and satellite communication — and also described the current progress in their experimental implementation. Although all these approaches can find their applications, the development of a quantum repeater based on solid-state systems is apparently of the greatest practical importance, because it would allow deploying quantum networks first on the scale of cities and then on the scale of countries and continents. The most recent results encourage that a fully functional quantum repeater will be created in the next decade.

Acknowledgments. I am grateful to N N Kolachevsky and P Barclay, and to my colleagues M Bhaskar, R Riedinger, E Bersin, Yu A Sukachev, S A Fedorov, and O V Belyaeva for their help in writing this review.

References

1. Poplavskii R P *Sov. Phys. Usp.* **18** 222 (1975); *Usp. Fiz. Nauk* **115** 465 (1975)
2. Manin Yu I *Vychislimoe i Nevychislimoe* (Computable and Non-computable) (Moscow: Sovetskoe Radio, 1980)

3. Feynman R P *Int. J. Theor. Phys.* **21** 467 (1982)
4. Deutsch D, Jozsa R *Proc. R. Soc. Lond. A* **439** 553 (1992)
5. Shor P W, in *Proc. of the 35th Annual Symp. on Foundations of Computer Science, 20 – 22 November 1994, Santa Fe, NM, USA* (Los Alamitos, CA: IEEE Computer Soc., 1994) p. 124
6. Rivest R L, Shamir A, Adleman L *Commun. ACM* **21** 120 (1978)
7. Moldovyan N A *Vvedenie v Kriptosistemy s Otkrytym Klyuchom* (Introduction to Cryptosystems with a Public Key) (Moscow: BHV, 2014) p. 228
8. Xu N et al. *Phys. Rev. Lett.* **108** 130501 (2012)
9. Gidney C, Ekerå M *Quantum* **5** 433 (2021); arXiv:1905.09749
10. Arute F et al. *Nature* **574** 505 (2019); arXiv:1910.11333
11. Bernien H et al. *Nature* **551** 579 (2017); arXiv:1707.04344
12. Zhang J et al. *Nature* **551** 601 (2017); arXiv:1708.01044
13. Diamanti E et al. *npj Quantum Inf.* **2** 16025 (2016); arXiv:1606.05853
14. Bernstein D J, Buchmann J, Dahmen E (Eds) *Post-Quantum Cryptography* (Berlin: Springer, 2009)
15. Bennett C H, Brassard G, in *Proc. of IEEE Intern. Conf. on Computers, Systems and Signal Processing* (New York: IEEE, 1984) p. 8
16. Gisin N et al. *Rev. Mod. Phys.* **74** 145 (2002); quant-ph/0101098
17. "Prodemonstrirovana rabota predseriinogo obraztsa pervogo v Rossii kvantovogo telefona" ("The work of a pre-production sample of the first quantum telephone in Russia is demonstrated"), press service of Lomonosov Moscow State University. 29.05.2019, https://www.msu.ru/science/main_themes/prodemonstrirovana-rabota-predseriynogo-obraztsa-pervogo-v-rossii-kvantovogo-telefona.html
18. Duplinskiy A V et al. *J. Russ. Laser Res.* **39** 113 (2018); arXiv:1712.09831
19. Wootters W K, Zurek W H *Nature* **299** 802 (1982)
20. Yin H-L et al. *Phys. Rev. Lett.* **117** 190501 (2016)
21. Briegel H-J et al. *Phys. Rev. Lett.* **81** 5932 (1998)
22. Duan L-M et al. *Nature* **414** 413 (2001); quant-ph/0105105
23. Kimble H J *Nature* **453** 1023 (2008); arXiv:0806.4195
24. Monroe C et al. *Phys. Rev. A* **89** 022317 (2014); arXiv:1208.0391
25. Fitzsimons J F *npj Quantum Inf.* **3** 23 (2017); arXiv:1611.10107
26. Barz S et al. *Science* **335** 303 (2012); arXiv:1110.1381
27. Gottesman D, Jennewein T, Croke S *Phys. Rev. Lett.* **109** 070503 (2012); arXiv:1107.2939
28. Khabiboulline E T et al. *Phys. Rev. Lett.* **123** 070504 (2019); arXiv:1809.01659
29. Dai H et al. *Nat. Phys.* **16** 848 (2020)
30. Kómár P et al. *Nat. Phys.* **10** 582 (2014); arXiv:1310.6045
31. Ilo-Okeke E O et al. *npj Quantum Inf.* **4** 40 (2018); arXiv:1709.08423
32. Krutyanskiy V et al. *npj Quantum Inf.* **5** 72 (2019); arXiv:1901.06317
33. Pirandola S et al. *Nat. Photon.* **12** 724 (2018); arXiv:1811.01969
34. Giovannetti V, Lloyd S, MacCone L *Phys. Rev. Lett.* **96** 010401 (2006); quant-ph/0509179
35. Degen C L, Reinhard F, Cappellaro P *Rev. Mod. Phys.* **89** 035002 (2017); arXiv:1611.02427
36. Vazirani U, Vidick T *Phys. Rev. Lett.* **113** 140501 (2014); arXiv:1210.1810
37. Belinskii A V, Klyshko D N *Phys. Usp.* **36** 653 (1993); *Usp. Fiz. Nauk* **163** (8) 1 (1993)
38. Wehner S, Elkouss D, Hanson R *Science* **362** eaam9288 (2018)
39. Lemonde M-A et al. *Phys. Rev. Lett.* **120** 213603 (2018)
40. Wang H, Lekavicius I *Appl. Phys. Lett.* **117** 230501 (2020); arXiv:2011.09990
41. Neuman T et al., arXiv:2003.08383
42. Magnard P et al. *Phys. Rev. Lett.* **125** 260502 (2020)
43. Aharonovich I, Englund D, Toth M *Nat. Photon.* **10** 631 (2016)
44. Eisaman M D et al. *Rev. Sci. Instrum.* **82** 071101 (2011)
45. Wang X et al. *Chem. Soc. Rev.* **45** 2239 (2016)
46. Senellart P, Solomon G, White A *Nat. Nanotechnol.* **12** 1026 (2017)
47. Wang H et al. *Nat. Photon.* **13** 770 (2019)
48. Zaske S et al. *Phys. Rev. Lett.* **109** 147404 (2012); arXiv:1204.6253
49. Ates S et al. *Phys. Rev. Lett.* **109** 147405 (2012); arXiv:1207.4226
50. Pelc J S et al. *Opt. Express* **20** 27510 (2012)
51. Takemoto K et al. *Sci. Rep.* **5** 14383 (2015)
52. Pirandola S et al. *Adv. Opt. Photon.* **12** 1012 (2020); arXiv:1906.01645
53. Scarani V et al. *Rev. Mod. Phys.* **81** 1301 (2009); arXiv:0802.4155
54. Hadfield R H *Nat. Photon.* **3** 696 (2009)
55. Bhaskar M K et al. *Nature* **580** 60 (2020)
56. Gol'tsman G N et al. *Appl. Phys. Lett.* **79** 705 (2001)
57. Marsili F et al. *Nat. Photon.* **7** 210 (2013); arXiv:1209.5774
58. Raussendorf R, Briegel H J *Phys. Rev. Lett.* **86** 5188 (2001)
59. Walther P et al. *Nature* **434** 169 (2005)
60. Chen K et al. *Phys. Rev. Lett.* **99** 120503 (2007); arXiv:0705.0174
61. CorningM SMF-28M Ultra Optical Fiber. Product Information, https://www.corning.com/media/worldwide/coc/documents/Fiber/SMF-28%20Ultra.pdf
62. Tamura Y et al. *J. Lightwave Technol.* **36** 44 (2018)
63. Takesue H et al. *Nat. Photon.* **1** 343 (2007)
64. Bennett C H et al. *Phys. Rev. Lett.* **70** 1895 (1993)
65. Żukowski M et al. *Phys. Rev. Lett.* **71** 4287 (1993)
66. Bose S, Vedral V, Knight P L *Phys. Rev. A* **57** 822 (1998); quant-ph/9708004
67. Pirandola S et al. *Nat. Commun.* **8** 15043 (2017); arXiv:1510.08863
68. Pirandola S *Commun. Phys.* **2** 51 (2019)
69. Hensen B et al. *Nature* **526** 682 (2015)
70. Rosenfeld W et al. *Phys. Rev. Lett.* **119** 010402 (2017); arXiv:1611.04604
71. Chou C-W et al. *Science* **316** 1316 (2007); quant-ph/0702057
72. Humphreys P C et al. *Nature* **558** 268 (2018); arXiv:1712.07567
73. Hofmann J et al. *Science* **337** 72 (2012)
74. Delteil A et al. *Nat. Phys.* **12** 218 (2016); arXiv:1507.00465
75. Yu Y et al. *Nature* **578** 240 (2020)
76. Monroe C, Kim J *Science* **339** 1164 (2013)
77. Devoret M H, Schoelkopf R J *Science* **339** 1169 (2013)
78. Awschalom D D et al. *Nat. Photon.* **12** 516 (2018)
79. Stern L et al. *Optica* **4** 1 (2017)
80. MacQuarrie E R et al. *Phys. Rev. Lett.* **111** 227602 (2013); arXiv:1306.6356
81. Arrangoiz-Arriola P et al. *Phys. Rev. X* **8** 031007 (2018)
82. DiCarlo L et al. *Nature* **460** 240 (2009); arXiv:0903.2030
83. Abobeih M H et al. *Nat. Commun.* **9** 2552 (2018)
84. DiVincenzo D P *Fortsch. Phys.* **48** 771 (2000)
85. Bennett C H et al. *Phys. Rev. Lett.* **76** 722 (1996); quant-ph/9511027
86. Borregaard J et al. *Phys. Rev. X* **10** 021071 (2020)
87. Lauk N et al. *Quantum Sci. Technol.* **5** 020501 (2020)
88. Mirhosseini M et al. *Nature* **588** 599 (2020); arXiv:2004.04838
89. Sangouard N et al. *Rev. Mod. Phys.* **83** 33 (2011); arXiv:0906.2699
90. Simon C et al. *Eur. Phys. J. D* **58** 1 (2010)
91. Blatt R, Roos C F *Nat. Phys.* **8** 277 (2012)
92. Gross C, Bloch I *Science* **357** 995 (2017)
93. Lekitsch B et al. *Sci. Adv.* **3** e1601540 (2017); arXiv:1508.00420
94. Duan L-M, Monroe C *Rev. Mod. Phys.* **82** 1209 (2010)
95. Colombe Y et al. *Nature* **450** 272 (2007)
96. Reichel J, Vuletić V (Eds) *Atom Chips* (Weinheim: Wiley-VCH, 2011)
97. Wang J et al. *Nat. Photon.* **14** 273 (2020)
98. Elshaari A W et al. *Nat. Photon.* **14** 285 (2020)
99. Purcell E M, Torrey H C, Pound R V *Phys. Rev.* **69** 37 (1946)
100. Bykov V P *Sov. J. Quantum Electron.* **4** 861 (1975); *Kvantovaya Elektron.* **1** 1557 (1974)
101. Reiserer A, Rempe G *Rev. Mod. Phys.* **87** 1379 (2015); arXiv:1412.2889
102. Brekenfeld M et al. *Nat. Phys.* **16** 647 (2020)
103. Albrecht R et al. *Phys. Rev. Lett.* **110** 243602 (2013)
104. Ruf M et al. *Phys. Rev. Appl.* **15** 024049 (2021); arXiv:2009.08204
105. Riedel D et al. *Phys. Rev. X* **7** 031040 (2017)
106. Choi H, Heuck M, Englund D *Phys. Rev. Lett.* **118** 223605 (2017)
107. Robinson J T et al. *Phys. Rev. Lett.* **95** 143901 (2005)
108. Giesz V et al. *Nat. Commun.* **7** 11986 (2016)
109. Mouradian S et al. *Appl. Phys. Lett.* **111** 021103 (2017)
110. Duan L-M, Kimble H J *Phys. Rev. Lett.* **92** 127902 (2004); arXiv:0309187
111. Najer D et al. *Nature* **575** 622 (2019)
112. Takahashi H et al. *Phys. Rev. Lett.* **124** 013602 (2020); arXiv:1808.04031
113. Stute A et al. *Nature* **485** 482 (2012)
114. Atatüre M et al. *Nat. Rev. Mater.* **3** 38 (2018)
115. Awschalom D D et al. *Nat. Photon.* **12** 516 (2018)
116. Zhang G et al., arXiv:2008.06458

117. Gruber A et al. *Science* **276** 2012 (1997)
118. Chu Y, Lukin M D, arXiv:1504.05990
119. Barry J F et al. *Rev. Mod. Phys.* **92** 015004 (2020); arXiv:1903.08176
120. Abobeih M H et al. *Nat. Commun.* **9** 2552 (2018); arXiv:1801.01196
121. Bradley C E et al. *Phys. Rev. X* **9** 031045 (2019); arXiv:1905.02094
122. Kalb N et al. *Science* **356** 928 (2017); arXiv:1703.03244
123. Faraon A et al. *Phys. Rev. Lett.* **109** 033604 (2012); arXiv:1202.0806
124. Udvarhelyi P et al. *Phys. Rev. Appl.* **11** 044022 (2019)
125. Ruf M et al. *Nano Lett.* **19** 3987 (2019)
126. Rozpedek F et al. *Phys. Rev. A* **99** 052330 (2019); arXiv:1809.00364
127. Ghobadi R et al. *Phys. Rev. A* **99** 053825 (2019)
128. Mills A R et al. *Nat. Commun.* **10** 1063 (2019); arXiv:1809.03976
129. Safonov A N et al. *Phys. Rev. Lett.* **77** 4812 (1996)
130. Hoese M et al. *Sci. Adv.* **6** eaba6038 (2020)
131. Dietrich A et al. *Phys. Rev. B* **101** 081401 (2020); arXiv:1903.02931
132. Vavilov V S et al. *Sov. Phys. Semicond.* **14** 1078 (1980); *Fiz. Tekh. Poluprovodn.* **14** 1811 (1980)
133. Zaitsev A M, Vavilov V S, Gippius A A *Kr. Soobshch. Fiz. FIAN* (10) 20 (1981)
134. Ekimov E A, Kondrin M V *Phys. Usp.* **60** 539 (2017); *Usp. Fiz. Nauk* **187** 577 (2017)
135. Wang C et al. *J. Phys. B* **39** 37 (2005)
136. Sipahigil A et al. *Science* **354** 847 (2016)
137. Nguyen C T et al. *Phys. Rev. Lett.* **123** 183602 (2019); arXiv:1907.13199
138. Evans R E et al. *Science* **362** 662 (2018); arXiv:1807.04265
139. Jahnke K D et al. *New J. Phys.* **17** 043011 (2015)
140. Sukachev D D et al. *Phys. Rev. Lett.* **119** 223602 (2017); arXiv:1708.08852
141. Goss J P et al. *Phys. Rev. B* **72** 035214 (2005)
142. Evans R E et al. *Phys. Rev. Appl.* **5** 044010 (2016); arXiv:1512.03820
143. Harris I et al. *Phys. Rev. B* **102** 195206 (2020); arXiv:1907.12548
144. Palyanov Yu N et al. *Sci. Rep.* **5** 14789 (2015)
145. Iwasaki T et al. *Sci. Rep.* **5** 12882 (2015)
146. Iwasaki T et al. *Phys. Rev. Lett.* **119** 253601 (2017); arXiv:1708.03576
147. Trusheim M E et al. *Phys. Rev. Lett.* **124** 023602 (2020)
148. Trusheim M E et al. *Phys. Rev. B* **99** 075430 (2019); arXiv:1805.12202
149. Kim S et al. *Nat. Commun.* **9** 2623 (2018); arXiv:1801.04399
150. Gottscholl A et al. *Nat. Mater.* **19** 540 (2020)
151. Jungwirth N R, Fuchs G D *Phys. Rev. Lett.* **119** 057401 (2017)
152. Tran T T et al. *Nat. Nanotechnol.* **11** 37 (2016)
153. Zargaleh S A et al. *Phys. Rev. B* **98** 165203 (2018)
154. Christle D J et al. *Phys. Rev. X* **7** 021046 (2017)
155. Bergeron L et al. *PRX Quantum* **1** 020301 (2020)
156. Bergeron L, Ph.D. Thesis (Burnaby, BC: Simon Fraser Univ., 2019)
157. Ekimov A I, Onushenko A A *JETP Lett.* **34** 345 (1981); *Pis'ma Zh. Eksp. Teor. Fiz.* **34** 363 (1981)
158. Lodahl P, Mahmoodian S, Stobbe S *Rev. Mod. Phys.* **87** 347 (2015); arXiv:1312.1079
159. Gross E F *Sov. Phys. Usp.* **5** 195 (1962); *Usp. Fiz. Nauk* **76** 433 (1962)
160. Press D et al. *Nat. Photon.* **4** 367 (2010)
161. Deng G-W et al., *Quantum Dot Optoelectronic Devices* (Lecture Notes in Nanoscale Science and Technology, Vol. 27, Eds P Yu, Z M Wang) (Cham: Springer Intern. Publ., 2020) p. 107
162. Veldhorst M et al. *Nat. Nanotechnol.* **9** 981 (2014); arXiv:1407.1950
163. Zajac D M et al. *Science* **359** 439 (2018)
164. Loss D, DiVincenzo D P *Phys. Rev. A* **57** 120 (1998); cond-mat/9701055
165. Novoselov K S et al. *Science* **353** aac9439 (2016)
166. Wang Q H et al. *Nat. Nanotechnol.* **7** 699 (2012)
167. Mak K F, Shan J *Nat. Photon.* **10** 216 (2016)
168. Keldysh L V *JETP Lett.* **29** 658 (1979); *Pis'ma Zh. Eksp. Teor. Fiz.* **29** 716 (1979)
169. Srivastava A et al. *Nat. Nanotechnol.* **10** 491 (2015)
170. Plechinger G et al. *Phys. Status Solidi Rapid Res. Lett.* **9** 457 (2015); arXiv:1507.01342
171. Childress L et al. *Phys. Rev. Lett.* **96** 070504 (2006)
172. Grib A A *Sov. Phys. Usp.* **27** 284 (1984); *Usp. Fiz. Nauk* **142** 619 (1984)
173. Bennett C H et al. *Phys. Rev. A* **53** 2046 (1996); quant-ph/9511030
174. Bennett C H et al. *Phys. Rev. A* **54** 3824 (1996); quant-ph/9604024
175. Shor P W *Phys. Rev. A* **52** R2493 (1995)
176. Terhal B M *Rev. Mod. Phys.* **87** 307 (2015); arXiv:1302.3428
177. Muralidharan S et al. *Sci. Rep.* **6** 20463 (2016)
178. Guha S et al. *Phys. Rev. A* **92** 022357 (2015); arXiv:1404.7183
179. Van der Wal C H et al. *Science* **301** 196 (2003)
180. Kuzmich A et al. *Nature* **423** 731 (2003); quant-ph/0305162
181. Yuan Z-S et al. *Nature* **454** 1098 (2008); arXiv:0803.1810
182. Zhao B et al. *Phys. Rev. Lett.* **98** 240502 (2007)
183. Jiang L, Taylor J M, Lukin M D *Phys. Rev. A* **76** 012301 (2007)
184. Wallraff A et al. *Nature* **431** 162 (2004)
185. Blais A et al. *Phys. Rev. A* **69** 062320 (2004); cond-mat/0402216
186. Häffner H et al. *Nature* **438** 643 (2005); quant-ph/0603217
187. Moehring D L et al. *Nature* **449** 68 (2007)
188. Monroe C et al. *Phys. Rev. Lett.* **75** 4714 (1995)
189. Meraner M et al. *Phys. Rev. A* **102** 052614 (2020); arXiv:1912.09259
190. Lo H-K, Curty M, Qi B *Phys. Rev. Lett.* **108** 130503 (2012); arXiv:1109.1473
191. Nguyen C T et al. *Phys. Rev. B* **100** 165428 (2019); arXiv:1907.13200
192. Varnava M, Browne D E, Rudolph T *Phys. Rev. Lett.* **97** 120501 (2006); quant-ph/0507036
193. Munro W J et al. *Nat. Photon.* **6** 777 (2012); arXiv:1306.4137
194. Fowler A G et al. *Phys. Rev. Lett.* **104** 180503 (2010); arXiv:0910.4074
195. Muralidharan S et al. *Phys. Rev. Lett.* **112** 250501 (2014); arXiv:1310.5291
196. Glaudell A N, Waks E, Taylor J M *New J. Phys.* **18** 093008 (2016)
197. Briegel H J, Raussendorf R *Phys. Rev. Lett.* **86** 910 (2001); quant-ph/0004051
198. Schwartz I et al. *Science* **354** 434 (2016); arXiv:1606.07492
199. Gimeno-Segovia M, Rudolph T, Economou S E *Phys. Rev. Lett.* **123** 070501 (2019); arXiv:1801.02599
200. Nielsen M A *Rep. Math. Phys.* **57** 147 (2006); quant-ph/0504097
201. Raussendorf R, Briegel H J *Phys. Rev. Lett.* **86** 5188 (2001)
202. Azuma K, Tamaki K, Lo H-K *Nat. Commun.* **6** 6787 (2015); arXiv:1309.7207
203. Lindner N H, Rudolph T *Phys. Rev. Lett.* **103** 113602 (2009)
204. He Y-M et al. *Nat. Nanotechnol.* **8** 213 (2013); arXiv:1303.4058
205. Lu C-Y et al. *Nat. Phys.* **3** 91 (2007)
206. Li Z-D et al. *Nat. Photon.* **13** 644 (2019); arXiv:1908.05351
207. Hasegawa Y et al. *Nat. Commun.* **10** 13480 (2020)
208. Lake D P et al. *Nat. Commun.* **11** 2208 (2020)
209. Armani D K et al. *Nature* **421** 925 (2003)
210. Akhmanov S A, Khokhlov R V *Sov. Phys. JETP* **16** 252 (1963); *Zh. Eksp. Teor. Fiz.* **43** 351 (1962)
211. Kroll H *Phys. Rev.* **127** 1207 (1962)
212. Kingston R H *Proc. IRE* **50** 472 (1962)
213. Boyd R *Nonlinear Optics* (New York: Academic Press, 2008) p. 640
214. Ashkin A, Boyd G, Dziedzic J *IEEE J. Quantum Electron.* **2** 109 (1966)
215. Houe M, Townsend P D *J. Phys. D* **28** 1747 (1995)
216. Tanzilli S et al. *Eur. Phys. J. D* **18** 155 (2002)
217. Zaske S et al. *Phys. Rev. Lett.* **109** 147404 (2012); arXiv:1204.6253
218. Dréau A et al. *Phys. Rev. Appl.* **9** 064031 (2018)
219. Hill J T et al. *Nat. Commun.* **3** 1196 (2012); arXiv:1206.0704
220. Dong C et al. *Science* **338** 1609 (2012)
221. Mitchell M, Lake D P, Barclay P E *Optica* **6** 832 (2019); arXiv:1902.07763
222. Lucamarini M et al. *Nature* **557** 400 (2018); arXiv:1811.06826
223. Ursin R et al. *Nat. Phys.* **3** 481 (2007)
224. Nauerth S et al. *Proc. SPIE* **8518** 85180D (2012)
225. Vallone G et al. *Phys. Rev. Lett.* **115** 040502 (2015); arXiv:1406.4051
226. Yin J et al. *Science* **356** 1140 (2017); arXiv:1707.01339
227. Buttler W T et al. *Phys. Rev. Lett.* **84** 5652 (2000); quant-ph/0001088
228. Schmitt-Manderbach T et al. *Phys. Rev. Lett.* **98** 010504 (2007)
229. Liao S-K et al. *Nat. Photon.* **11** 509 (2017)
230. Fedrizzi A et al. *Nat. Phys.* **5** 389 (2009)
231. Yin J et al. *Nature* **488** 185 (2012); arXiv:1205.2024
232. Bedington R, Arrazola J M, Ling A *npj Quantum Inf.* **3** 30 (2017); arXiv:1707.03613
233. Nauerth S et al. *Nat. Photon.* **7** 382 (2013)
234. Boone K et al. *Phys. Rev. A* **91** 052325 (2015); arXiv:1410.5384
235. Yin J et al. *Nature* **582** 501 (2020)
236. Ekert A K *Phys. Rev. Lett.* **67** 661 (1991)

237. Joshi S K et al. *New J. Phys.* **20** 063016 (2018)
238. Rideout D et al. *Class. Quantum Grav.* **29** 224011 (2012)
239. Zhang Q et al. *Opt. Express* **26** 24260 (2018)
240. Sasaki M et al. *Opt. Express* **19** 10387 (2011)
241. Dynes J F et al. *npj Quantum Inf.* **5** 101 (2019)
242. Kiktenko E O et al. *Quantum Electron.* **47** 798 (2017); *Kvantovaya Elektron.* **47** 798 (2017); arXiv:1705.07154
243. Stepanova Yu "Kvanty stavyat na rel'sy. V OAO RZhD otsenili sozdanie novoi seti peredachi dannykh" ("Quanta are put on the rails. Russian Railways assessed the creation of a new data transmission network"), Kommersant 13.01.2020; https://www.kommersant.ru/doc/4219027
244. Liao S-K et al. *Phys. Rev. Lett.* **120** 030501 (2018); arXiv:1801.04418
245. Aharonov Y, Zubairy M S *Science* **307** 875 (2005)
246. Pfleegor R L, Mandel L *Phys. Rev.* **159** 1084 (1967)
247. Minder M et al. *Nat. Photon.* **13** 334 (2019); arXiv:1910.01951
248. Zhong X et al. *Phys. Rev. Lett.* **123** 100506 (2019); arXiv:1902.10209
249. Wang X-B, Yu Z-W, Hu X-L *Phys. Rev. A* **98** 062323 (2018)
250. Liu Y et al. *Phys. Rev. Lett.* **123** 100505 (2019); arXiv:1902.06268
251. Fang X-T et al. *Nat. Photon.* **14** 422 (2020)